Journal of Cleaner Production 365 (2022) 132702

Contents lists available at ScienceDirect

Journal of Cleaner Production

journal homepage: www.elsevier.com/locate/jclepro

Spotlighting graphene-based catalysts for the mitigation of environmentally hazardous pollutants to cleaner production: A review

Yasser Vasseghian [a], Van Thuan Le [b,c], Sang-Woo Joo [a,*], Elena-Niculina Dragoi [d], Hesam Kamyab [e,f,**], Shreeshivadasan Chelliapan [g], Jiří Jaromír Klemeš [h]

[a] Department of Chemistry, Soongsil University, Seoul, 06978, South Korea
[b] Center for Advanced Chemistry, Institute of Research and Development, Duy Tan University, 03 Quang Trung, Da Nang, 55000, Viet Nam
[c] The Faculty of Natural Sciences, Duy Tan University, 03 Quang Trung, Da Nang, 55000, Viet Nam
[d] Faculty of Chemical Engineering and Environmental Protection "Cristofor Simionescu", "Gheorghe Asachi" Technical University, Iasi, Bld Mangeron No 73, 700050, Romania
[e] Malaysia-Japan International Institute of Technology Universiti Teknologi Malaysia, Jalan Sultan Yahya Petra, 54100, Kuala Lumpur, Malaysia
[f] Department of Biomaterials, Saveetha Dental College and Hospital, Saveetha Institute of Medical and Technical Sciences, Chennai, 600 077, India
[g] Engineering Department, Razak Faculty of Technology and Informatics, Universiti Teknologi Malaysia, Jln Sultan Yahya Petra, 54100, Kuala Lumpur, Malaysia
[h] Sustainable Process Integration Laboratory (SPIL), NETME Centre, Faculty of Mechanical Engineering, Brno University of Technology - VUT Brno, Technická 2896/2, 616 00, Brno, Czech Republic

ARTICLE INFO

Handling Editor: Cecilia Maria Villas Bôas de Almeida

Keywords:
Graphene-based catalysts
Nanocatalysts
Cleaner production
Hazardous pollutants
Degradation

ABSTRACT

In recent years, population growth and industrial development have raised concerns about environmental pollution and had negative effects on the entire ecosystem. Cleaner production is an effective strategy to reduce these negative effects and prevent damage to the environment. Graphene (GR)-based catalysts as eco-friendly catalysts for the mitigation of environmentally hazardous pollutants, such as pollutant degradation, CO_2 reduction, and air purification, have been introduced as one of these cleaner production strategies. In this review, the benefits of GR-based catalysts for the breakdown of organic contaminants are highlighted. Besides, critical considerations, potential solutions, challenges, and upcoming development opportunities for GR-based catalysts in sustainable applications were discussed. The main observations are: (i) GR-based catalysts are different types, and there are several methods to synthesize them, (ii) GR-based catalysts are efficient catalysts for the mitigation of environmentally hazardous pollutants, and (iii) several issues must be resolved for the broad applicability of GR-based catalysts, namely, a) unclear mechanisms and/or lack of a basic understanding of the function of GR; b) complex problems related to the preparation of GR; c) graphene's derivates on a large scale; d) finite stability in specific reactions (e.g., photocatalysis); and e) development of synthetic methods for producing large quantities of high-quality GR nanomaterials. Accordingly, the research and development space has clearly shown that GR-based nanomaterials are the basis for future catalysts for cleaner production.

1. Introduction

Since the discovery of graphene (GR) (Chen et al., 2020), the nano-structured carbon allotrope GR has captured the attention of both scientists and engineers (Vasseghian et al., 2022) which has been shown to have an incredible ability to improve many materials, extending their applicability and efficiency. GR, one of the thinnest materials known to humans, consists of carbon atoms structured in a single-layer 2-dimensional sheet. These carbon atoms, organised in a hexagonal pattern with sp^2 hybridised configuration, have high efficiency when used in various systems (Mahdiani et al., 2018).

GR is extraordinarily strong, roughly 200 fold stronger than steel, and it is a good heat and electrical conductor and has an unusual capacity to absorb light. It's also tougher than diamond, more flexible than rubber, and less heavy than aluminium. Experiments show that GR is also elastic so that it can be stretched 20–25% longer without breaking

* Corresponding author. Department of Chemistry, Soongsil University, Seoul, 06978, South Korea.
** Corresponding author. Malaysia-Japan International Institute of Technology Universiti Teknologi Malaysia, Jalan Sultan Yahya Petra, 54100, Kuala Lumpur, Malaysia.
E-mail addresses: sjoo@ssu.ac.kr (S.-W. Joo), khesam2@live.utm.my (H. Kamyab).

https://doi.org/10.1016/j.jclepro.2022.132702
Received 11 April 2022; Received in revised form 28 May 2022; Accepted 12 June 2022
Available online 15 June 2022

it. The reason for this was the flexibility of the carbon atoms in GR (Le et al., 2021). Other properties of GR include the high mobility of its electrons, which are 100 times faster than silicon (Raccichini et al., 2015). GR conducts heat twice as well as diamond and has 13 times better electrical conductivity than copper, and absorbs only 2.3% of the reflected light (Buron et al., 2015). The transparency of GR also gives it unique optical properties as an atomic monolayer (Ding et al., 2015). A single-layer GR plate has a surface area of 2,630 $m^2\ g^{-1}$ and is impermeable, allowing not even the tiniest atom (helium) to pass through. It also represents a new class of one-atom-thick materials known as two-dimensional materials since they only expand in two dimensions, length and width. (Ding et al., 2015). GR is also used to make mixed heterogeneous van der Waals structures that can, by GR hybridisation with 0-dimensional quantum dots or nanoparticles, produce one-dimensional nanostructures such as nanowires or carbon nanotubes, or highly attractive three-dimensional bulk materials (Kumar et al., 2015).

The characteristics of GR, including both properties and structure, indicate that GR is well suited for various applications. Among the most important applications of GR in recent years were in separation (An et al., 2016), environments (Guo et al., 2021) (Fig. 1), transparent conducting electrodes (Kang et al., 2021), dye-sensitized solar cells (Mahalingam et al., 2021), sensors (Moon et al., 2021), supercapacitors (Lee et al., 2021), fuel cells (Jin et al., 2021), catalysts (Jiang et al., 2021), and even medicine (Valencia et al., 2021).

GR and its derivatives can be utilized as catalysts or catalytic supports because of their good specific surface area, high adsorption capacity, and superior biocompatibility (Wang et al., 2020). GR-based compounds can be effectively applied in a variety of reactions, including oxygen reduction (Guo et al., 2020) to CO_2 reduction (Pan et al., 2020), catalytic purification of volatile organic compounds (Wu et al., 2020), water treatment, and wastewater treatment (Yin et al., 2020). A vast number of reviews have been made to support this point. Hu et al. (2017) covered the synthesis pathway, characterisation approach and application of GR-based nanomaterials for catalysis. It was concluded that GR-based nanomaterials could serve as emerging catalysts in energy-related reactions, water splitting, photocatalysis, photoelectracatalysis, and environment-related reactions. Nidheesh et al. (Nidheesh, 2017) reported a review on GR-based materials that supported advanced oxidation processes for water and wastewater treatment. The work focused specifically on elucidating the performance-enhancing mechanism of advanced oxidation processes in the presence of GR-based catalysts. Furthermore, the progress, mechanisms and challenges of GR application in Fischer–Tropsch synthesis, water splitting, water treatment and oxygen reduction reaction have also been summarized by Yan et al.. However, there has been a lack of a systematic understanding of GR-based catalysts for the mitigation of environmentally hazardous pollutants to cleaner production (Yan et al., 2021).

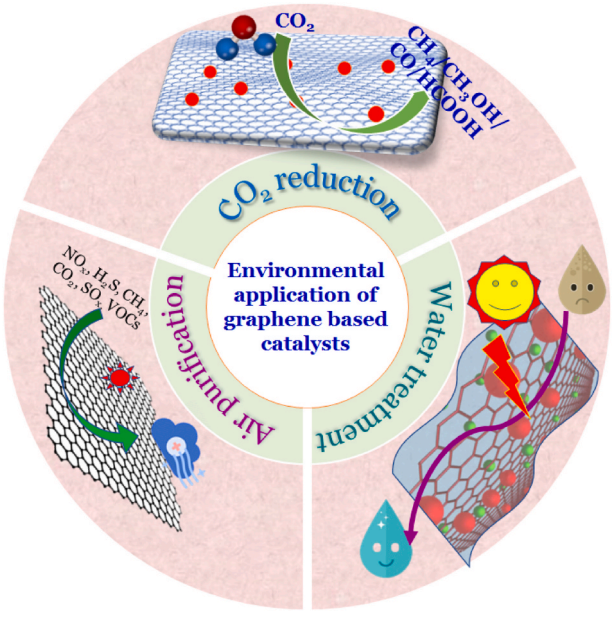

Fig. 1. Environmental applications of GR-based catalysts. This schematic illustrates that GR can act as the catalytic centre of a catalyst.

In this context, GR-based catalysts are revolutionary materials in the catalysis and chemistry communities (Saleh and AL-Hammadi, 2021). This study focuses on recent developments in GR-based nanocatalysts and discusses the key aspects of preparation, characterisation, and application. Furthermore, the environmental applications of GR are rigorously analyzed within the context of tightening environmental rules. Challenges and future research directions are also discussed. This review provides important information to the catalysis community to develop novel GR-based nanomaterials with superior catalytic efficiency.

2. Advantages and disadvantages of graphene as a catalyst

As a type of carbon with high electron mobility and a particular surface area, GR is an obvious option for use as catalytic support (Shandilya et al., 2018). In the most popular catalytic reactions, a noble metal catalyst is linked to support that acts as a mechanical support and facilitates the reaction by enabling charge transfer (Malinga and Jarvis, 2020). Because there are no free chemical connections in GR, in its purest form, it has a chemically inert surface. However, adding strain, defects, or functional groups to GR significantly changes its chemical characteristics, making it appropriate for use as catalytic support (Cherian et al., 2021).

Forming a covalent link between the solid support and the ligand binder is a preferred strategy for stabilizing metal complexes (Fadil et al., 2022). This standard technique has two significant limitations in the case of GR. The first is due to the requirement for additional factorization of the metal complex and GR's solid surface (which increases the cost of catalyst preparation), while the second is due to the possibility of changes in the chemical reactivity attributed to the formation of covalent bonds (Li et al., 2019).

As an alternative, non-covalent interactions are proving to be quite effective at generating supported catalysts without chemically modifying the homogeneous catalyst or the GR. Van der Waals forces and π-stacking are the most frequently encountered non-covalent interactions in hydrogen bonding (Hussain et al., 2022). While a single non-covalent interaction has far lower relative energy than a normal covalent bond, their cumulative influence on the metal complex's anchoring on the GR surface should not be negligible (Magne et al., 2021).

Gnana Kumar et al. (2014) produced platinum nanoparticles on a polymer/GR substrate for use as an anode catalyst in microbial fuel cells. Polyaniline (PANI) acts as a bridge between reduced graphene oxide (rGO) and Pt nanoparticles *via* electrostatic interaction, π- π stacking force, hydrogen bonding, and the Pt–N bond, thus increasing the intrinsic stability of the rGO/PANI/Pt composite. When compared to the manufactured rGO/PANI and rGO/Pt composites, the electrocatalytic performance of rGO/PANI/Pt demonstrated a higher oxidation current and a lower internal resistance (Gnana Kumar et al., 2014).

The ease of design and availability of a homogeneous catalyst immobilised via non-covalent interactions are key advantages (Oswal et al., 2022). Adjusting the electrical and spatial features allows for even more adjustments to obtain great selectivity and stability. For catalytic applications, well-supported molecular complexes should facilitate an accurate characterisation of hybrid materials and make the research of reaction an easier process (Lopes et al., 2021). With well-defined homogeneous organic metal methods, the reaction process can be

examined in solution at the molecular level. During the catalytic process, the support may have a role in boosting catalytic activity by preventing aggregation and encouraging contact between substrates and active catalytic species, rather than just anchoring the molecular complex (Zaera, 2022).

Because the number of functional groups in GR is restricted, non-covalent interactions employing π -stacking offer an appealing technique to stabilize metal complexes. Non-covalent contacts between the catalyst and the support are also emerging as a good alternative to the more extensively used covalent interactions, as they inhibit the working of the catalyst and the surface, potentially resulting in new properties for both catalysts and GR (Verma et al., 2022).

Under mild reaction conditions, non-covalent interactions bind Pd (Ma et al., 2015) and Ru (Liu et al., 2011) metal complexes to the GR surface. The findings indicate that the metal complexes are firmly fixed on the surface of GR. The catalytic capabilities of the hybrid material show that when the metal complex is stable on the GR surface, the catalytic activity increases. This system is reliable and may be used multiple times without lowering activity (Nagarajan et al., 2022).

Wei et al. synthesized palladium catalysts with GR support for highly selective hydrogenation of 1,3-cyclohexanedione (1,3-CHD) through giant π-conjugate interactions. Because there is a continuous π-π interaction force between GR nanosheets and resorcinol, and such an interaction force disappears when RES loses its aromatic property following the addition of the first H_2, the intermediate product with only one H_2 molecule, i.e., the enol isomer is added. In this study, 1,3-CHD was desorbed from the GR surface, and high selectivity was obtained. After simple washing with ordinary solvents, the Pd catalyst supported by GR was used several times (Wei et al., 2015).

Cao et al. synthesized one-step Ru nanoparticles on GR as a catalyst for ammonia borane hydrolytic dehydrogenation. GR-supported Ru nanoparticles were produced in a single step using methylamine borane as the reducing agent. The results of this work demonstrated that when metal complexes are attached to the surface of GR, their catalytic activity rises. Ru/GR nanoparticles outperformed their GR-free counterparts in catalyzing hydrolytic dehydrogenation (Cao et al., 2013).

A study by Akshatha et al. (2020) demonstrated the importance of metal complexes attached to the GR surface via non-covalent interactions, using rutile, mesoporous ruthenium oxide decorated graphene oxide (GO) as a visible-light-driven photocatalyst for hydrogen evolution. The complex's catalytic properties show that when the metal complex is stable on the surface of GR, the catalytic activity increases. The proposed system was dependable and reusable (Akshatha et al., 2020).

The main disadvantages of GR as a #catalyst are its high hydrophobicity and susceptibility to oxidative environments, leading to limited dispersion and its stability in aqueous media (Yam et al., 2020). Moreover, with the large electrical conductivity and no bandgap, it is difficult to use GR as a photocatalyst, and several derivatives of GR, such as GO, reduced GO (rGO), and doped GR, have been intensively explored in an attempt to further improve the application of GR in heterogeneous catalysis (Fig. 2) (Razaq et al., 2022). The oxygen functional groups present in both GO and rGO can enhance the solubility, dispersibility and stability of GR and provide the possibility of further modification with other functional groups. Nevertheless, the existence of oxygen-containing functional groups on the surface can create defects in the basal plane and electron irradiation on GR layers, reducing the mobility of electrons, conductivity, and catalytic activity (Yan et al.,

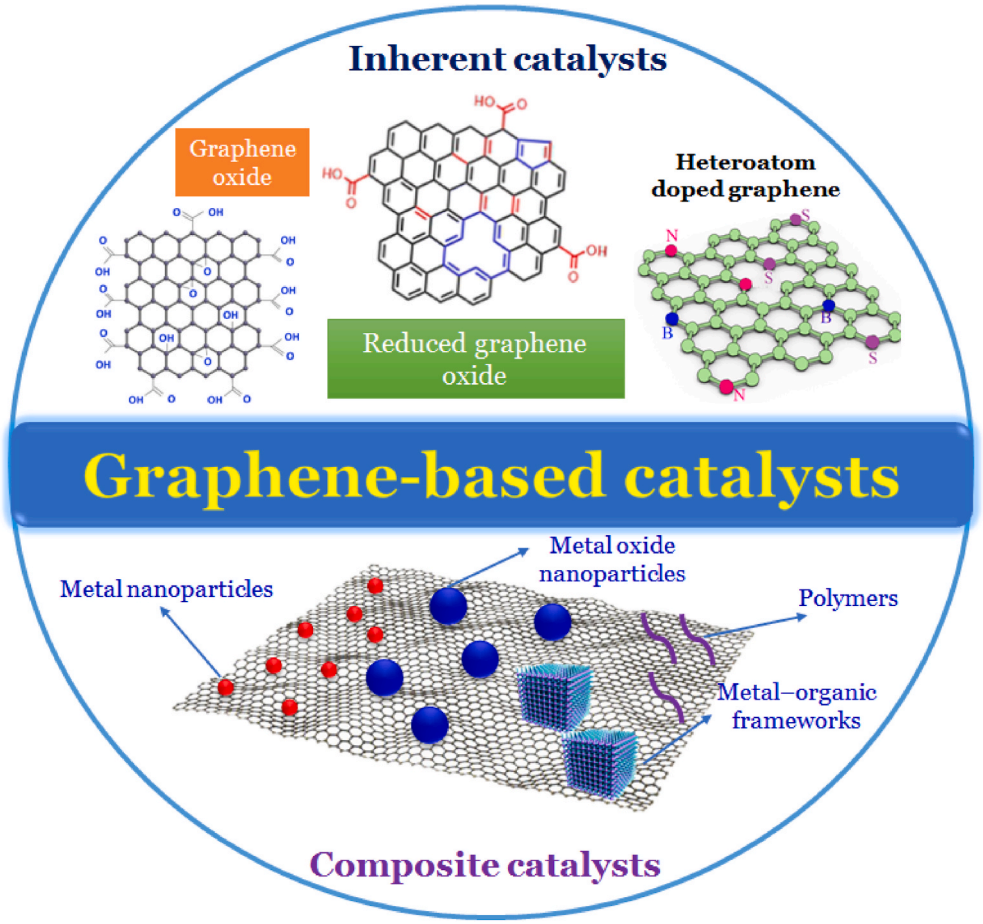

Fig. 2. Schematic of GR-based composite catalysts. GR and its allotropes can be composited with different structures and improve the efficiency of environmental processes.

2021). Up to now, efforts to improve the shortcomings of GR-based catalysts have not stopped.

3. Synthesis of the catalysts

GR-containing catalysts can be categorized into (*i*) inherently pure GR materials, such as GO, rGO, and heteroatom-doped GR; and (*ii*) composites in which GR is blended with other catalysts (Fig. 2). For pure GR, the catalytic activity is determined by the composition and structure of the sheets, whereas life duration is determined by morphological and structural stability (Scheuermann et al., 2009). In specific cases, inherently pure GR materials behave like homogenous polymer catalysts (Huang et al., 2012) and can be synthesized via a wet chemical approach, chemical vapour deposition (CVD), or GR post-treatment to yield composites (Wani et al., 2020). In composites, the role of GR is primarily to function as a conductive substrate that immobilizes the other components. The performance of a composite is related to the inherent qualities of the components and their interfacial interaction and/or synergistic effect (Sharma and Pollet, 2012). In most cases, composites are insoluble and behave like heterogeneous catalysts (Dreyer and Bielawski, 2011), and their life span is dependent on the catalyst immobilization and the GR stability (Scheuermann et al., 2009). The most useful strategies for preparing composites include mixing and *in situ* growth.

3.1. Inherent catalysts

3.1.1. Graphene oxide

GO is widely synthetised by graphite oxide exfoliation (Kumar et al., 2020). The thickness of a GO sheet was determined to be around 1 nm (Bai et al., 2011). The oxygenated groups from the GO structure raise lead to a thickness three higher than that of a pure GR sheet. Moreover, the introduction of oxygenated groups leads to the destruction of the conjugated structure of graphite. GO sheets can be dispersed in water or a polar organic solvent (Bond and Thompson, 1999). Additionally, a heavily oxidised GO is an insulator.

Several alterations to the Hummers' method were proposed to change the GO sheet's characteristics (size, properties, and composition) (Li et al., 2018). For instance, the productivity of GO was enhanced by pre-oxidising graphite with P_2O_5 and $K_2S_2O_8$ in H_2SO_4 (Kovtyukhova et al., 1999). The common oxidation methods for GO fabrication are summarized in Fig. 3.

3.1.2. Reduced graphene oxide

Chemical reduction of GO in a solid or dispersion state is the most often used method for creating rGO. In this case, various inorganic or organic compounds can be used (Hu et al., 2015) (Table 1). Many of the reducing agents that can be used are toxic or tough to handle for large scale generation. Reductive metals (iron, zinc) were applied as reducing agents for GO reduction (Naik et al., 2020). As these reductive acids are used at room temperature, this strategy is considered a green method for rGO production. Green tea is another method for obtaining rGO from GO. The tea contains polyphenol, a compound that interacts strongly with the sheets of rGO, resulting in a stable rGO dispersed in both aqueous and organic solvents (Agarwal and Zetterlund, 2020). Because they have more conjugated domains and a higher hydrophobic characteristic compared with their GO precursors, and because they have p-stacking and hydrophobic interactions, the rGO sheets usually form

Table 1
Reduction methods for rGO synthesis.

Reductants	Reduction conditions	C/O ratio	Ref.
Carbonic acid	22.73 M H_2CO_3, 100 °C, 3 h	10.45	Wadekar et al. (2018)
Caffeic acid	GO:Caffeic acid of 1:0.1, 180 °C, 24 h	5.99	Barra et al. (2021)
Amomonia borane	10 mg NH_3BH_3, room temperature, 1 h	9.6	Zhuo et al. (2015)
Sodium triacetoxy borohydride	6.57 mM $NaBH(Oac)_3$, 70 °C, 2 h	2.24	Chua and Pumera (2013)
Sodium borohydride	150 mM $NaBH_4$, 80 °C, 24 h	6.9	KF and Andersson (2017)
Phenylhydrazine	199.45 mM $C_6H_8N_2$, 25 °C, 24 h	9.51	Pham et al. (2010)
Hydrazine monohydrate	0.128 mM $N_2H_4{\cdot}HO_2$	10.3	(Stankovich et al.)
Potassium hydroxide	53.33 mM KOH, 50–90 °C	-	Fan et al. (2008)
Sodium hydroxide	53.33 mM NaOH, 50–90 °C	-	Fan et al. (2008)
Hydrogen bromide	143.99 mM HBr, 110 °C, 24 h	3.9	Chen et al. (2011)
Hydroiodic acid	0.06–0.95 M HI, 90 °C, 4 h	-	Liu and Speranza (2021)
Green tea	10 mL green tea (2g/50 mL H_2O), 60 °C, 6 h	-	Vatandost et al. (2020)
Vitamin C	1 mg/mL Vatamin C, 65 °C, 50 min	4.0	De Silva et al. (2018)

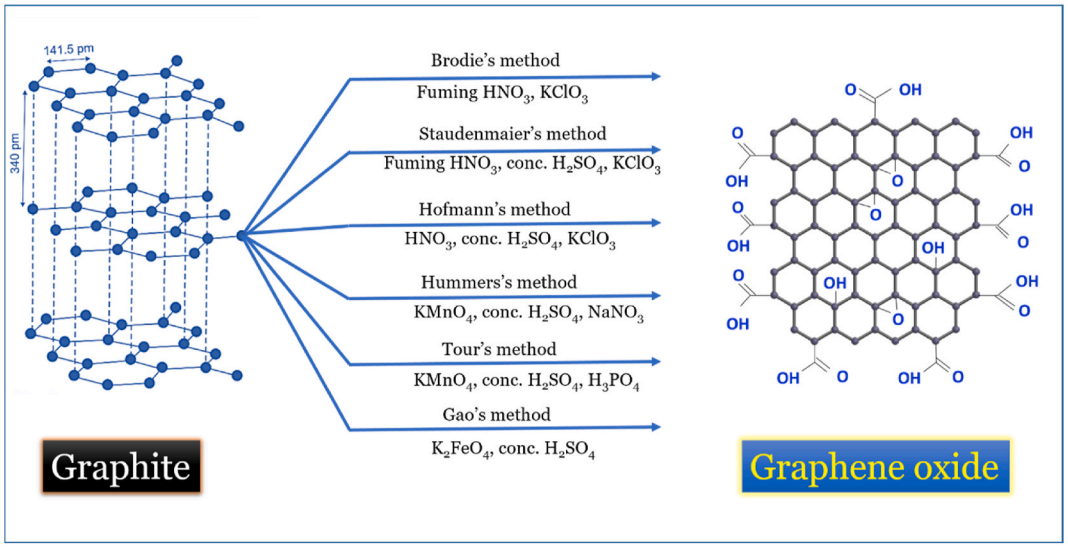

Fig. 3. Schematic diagram of GO synthesis from graphite.

irregular precipitates (Jakhar et al., 2020).

Strategies for producing (on a large scale) rGO with few residual oxygenated groups include a microwave-assisted thermal, thermal, hydrothermal or solvothermal reduction (Sun et al., 2021). Electrochemical reduction of GO can be used to create films of rGO with specific profiles or patterns (Bu et al., 2020). Additionally, the application of a laser beam or light flash on GO films can produce patterned rGO films (El-Kady et al., 2012).

3.1.3. Heteroatom doped graphene

Heteroatom-doping is a process in which the heteroatoms (boron, sulfur, oxygen, phosphor, nitrogen, etc.) replace some carbon atoms in the graphitic structure. The introduction of heteroatoms into graphitic carbon networks can lead to significant alteration of the physicochemical, electronic, and catalytic properties of GR due to the difference in size and electronegativity between heteroatoms and carbon atoms (Hu et al., 2018). Heteroatom dopants can be electron donors (e.g., N, P, S) or electron acceptors (e.g., B, F, I, Si) (Deokar et al., 2022). Among them, N and B are the most popular because they have similar sizes and valence electron numbers as carbon, so they are easily substituted into GR (Ma et al., 2021). There are mainly two approaches for fabricating heteroatom-doped GR, *i.e.*, *in situ* growth and post-treatment. The advantages and disadvantages of different methods used for the preparation of heteroatom doped GR and corresponding examples are presented in Table 2.

3.1.3.1. In-situ growth. In the *in-situ* growth method (belonging to the "bottom-up" class), the heteroatoms substitute carbon atoms and dope into the carbon framework during the GR growth. This procedure does not change the intrinsic GR properties and provides additional catalytic properties (Wu, Z. et al., 2019). The promising technique for this purpose is CVD, in which the GR films are prepared by a catalytic growth mechanism (Huet et al., 2020). In CVD, a metal catalyst (e.g., Cu or Ni) is used as the substrate; and the doping is occurred by mixing precursors (solid, liquid, or gaseous) containing desired heteroatom atoms with the gaseous carbon sources together in the growth furnace at a high temperature. The mixture then tends to dissociate and try to recombine by precipitation into the heteroatom-GR (Maharubin et al., 2016). The CVD method enables a reproducible and controlled high-quality synthesis of continuous, defect-free, single- or several-layer GR films at a large scale and low cost. For example, Son et al. (2020) developed a two-step (nucleation and lateral growth steps) CVD technique for fabricating

Table 2
Summary of the advantages and disadvantages of some synthesis methods for heteroatom doped GR and corresponding examples.

Methods	Advantages	Disadvantages	Doping heteroatom	Precursors	Target application	Ref.
CVD	Controlled quality and layer number; simultaneous growth and large-area preparation;	sophisticated instrumentation, high operating temperature; low-yields and high cost; needs transfer on a non-conducting substrate	N	Pyridine	CMOS logic devices, back-end interconnects, and flexible devices	Son et al. (2020)
			B	Diborane and methane	opto-electronic devices	Zan et al. (2021)
			S	Thiophene	supercapacitor electrode	Jeon et al. (2021)
			B, N	Methane and borazane	NO_2 gas sensor	Srivastava et al. (2022)
			S, N	Methane and phenothiazine	The catalyst for oxygen evolution reaction	Zhou et al. (2019)
Ball milling	Simple and scalable process; industrial-scale productivity	Difficult to control the doping process; doping only at the edges	N	Graphite and melamine	The catalyst for the oxygen reduction reaction	Dan et al. (2021)
			N	GO and melamine	The catalyst for the oxygen reduction reaction	Zhuang et al. (2017)
			S	Graphite and sulfur	Electrochemical catalysis	Chua et al. (2016)
			Sn	Graphite and Sn powder	Epoxy resin	Chen et al. (2022)
Solvothermal synthesis	Cheap equipment; easy operation; low temperature	lengthy processes; harsh feedstock; crumpled sheets; the yield is limited by the container; no control on GR layer number and flake size	N, B	GR, ammonia, and boron trioxide	pseudo-capacitive energy storage	Bhushan et al. (2020)
			S	DMSO and NaOH	Sodium-Ion Batteries	Quan et al. (2018)
Pyrolysis	Large-quantity production, abundant feedstock; cheap equipment; high crystalline product	High-temperature annealing; defective; lengthy processes; porous and powdered material	N	Ammonium acetate	Oxygen reduction reaction	Hassani et al. (2018)
			N, S	Thiourea and GR	Hydrogen evolution	Liu et al. (2019)
Arc discharge	Mass-production; simple operation; adjustable atmosphere and pressure;	low doping level; high voltage or current required; expensive equipment; mainly multilayer GR.	N	Graphite powder, GO, and PANI	Supercapacitor	Pham et al. (2019)
			F	Hollow graphite rod filled with powdery graphite fluoride	Batteries, low surface energy coatings and lubricants	Shen et al. (2012)
Thermal annealing	Controllable doping; cheap equipment; easy operation; wide choices of dopant precursors (gases, liquids, or solids); high efficiency	The high temperature required; partial functionalization occurs	N	Thermal annealing of fluorinated GO under the atmosphere of ammonia	Supercapacitor electrode	Jiang et al. (2019)
			B	GO and g-B_2O_3	Supercapacitor electrode	Yeom et al. (2015)
Hydrothermal synthesis	Low-cost; low-temperature (~200 °C), easily achieve doping and decoration; large-scale production;	No control on layer number and flake size; long synthesis process;	N, S	Go and methionine	Supercapacitor electrode	(Wu, D. et al., 2019)
Plasma	Low power consumption; short reaction time and	Low yield	N	Ethanol and ammonia	Supercapacitor	Bundaleska et al. (2018)

large-area, continuous N-doped GR films from a pyridine feedstock under ambient pressure at 300 °C. This method allowed to obtain large-area, continuous N-doped GR films of excellent quality: optical transmittance of 97.6%, the electron mobility of 1,400 $V^{-}1\ s^{-1}$, and a film size of 2 in (Son et al., 2020). Ullah et al. successfully designed a facile, controlled-flow CVD process to prepare high-quality and large-area monolayer Al-doped GR, which exhibited CO_2 capturability superior to those of other substitutionally doped GRs (Ullah et al., 2022).

3.1.3.2. Post-treatment. The post-treatment technique involves the incorporation of heteroatoms into the GR structure. This is accomplished by chemically or physically treating GR materials with heteroatom-containing compounds. N-doped GR, for example, can be synthesized by annealing GO in an NH_3 flow at temperatures varying from room temperature to 1,100 °C (Li et al., 2009). Other methods for obtaining N-doped GR nanoribbons include electrochemical reaction or thermal annealing of GR nanoribbons in an ammonia atmosphere (Wang et al., 2009). Various sources can be used as nitrogen atoms. Among ammonia, other nitrogen-rich organic compounds are: melamine (nitrogen content of about 66 wt% (Gayathri et al., 2019)), dicyandiamide, pyrimidine-2, 4,5,6-tetramine-sulphuric acid hydrate, pyrrole (Keramatinia et al., 2021).

3.2. Composite catalysts

3.2.1. Graphene/metal nanoparticle composites

The preparation of composites containing GR/metal nanoparticles usually requires to GO and metal salts (Phan et al., 2020). The first step in obtaining these materials is preparing a composite from metal ions and GO. Next, the composite undergoes a reduction treatment. This procedure allows the synthesis of various composites containing GR/metal nanoparticles. In the case of preparing Pd/rGO by reducing an in water (Scheuermann et al., 2009), first, a mixture of GO and palladium acetate with water was prepared. The mixture was put for 5 min under sonication and kept overnight to allow ion exchange. The obtained composite led to Pd/rGO by applying a decrease with hydrogen gas or hydrazine hydrate or heating treatment at 500–600 °C. For preparing Au/rGO, NaOH rGO was used as starting material (Li et al., 2012).

3.2.2. Graphene/metal oxide composites

Various metal salts included in GR can be changed to metal oxides to form composites containing rGO/metal oxide. GR/oxide composites can also be obtained through the hydrolysis of the metal salts found in systems containing GR-based compounds. For instance, TiF_4 can be hydrolszed in an aqueous dispersion of GO (or rGO), resulting in a TiO_2/GO (or TiO_2/rGO) composite (Lambert et al., 2009). The assembly of TiO_2 nanoparticles on GO sheets is influenced by the concentration of GO and by the mechanical stirring. TiO_2/rGO nanocomposite can also be obtained by using $TiCl_4$ as a precursor (Zhang et al., 2012).

Another approach to obtaining GR/metal oxide materials is to simply mix the two components. Mixing TiO_2 with GO dispersion (with an H_2O to ethanol ratio of 2: 1) represents one such example (Kanjwal et al., 2019). After that, to convert GO to rGO, the obtained mixture can be treated hydrothermally at 120 °C for 3 h, annealed at high temperatures, or can undergo a microwave-hydrothermal method.

3.2.3. Other graphene-based composite catalysts

In addition to metals and their oxides, many other catalysts can be mixed with GR to generate the composites. One effective strategy for the preparation of these composited is through self-assembly. For example, GO was reduced with $NaBH_4$ in the presence of polydiallyldimethylammoniumchloride to obtain a polydiallyldimethylammoniumchloride functionalised/adsorbed GR catalyst (Park et al., 2011).

Another strategy is to use one-step hydrothermal or solvothermal reactions. For example, through a hydrothermal treatment of a mix of rGO (as a scaffolding base) and ZnSe-$(diethylenetriamine)_{0.5}$, an N-doped GR/ZnSe nanocomposite was obtained (Chen et al., 2012).

4. Environmental applications of graphene-based catalysts toward cleaner production

4.1. CO_2 reduction

Converting greenhouse gases using CO_2 reduction represents a potentially green strategy that can alleviate the energy and, consequently, environmental problems that have been currently faced (Hasani et al., 2020). In the latest years, this has been achieved through complex strategies that are based on thermal, electrochemical, photochemical, and photo-electro-catalytic methods. In this context, the development and improvement of high-performance catalysts are critical because it has the potential to significantly reduce pollution. This section discusses recent advances in the use of GR-based catalysts, with a particular emphasis on simple or modified GR.

rGO was used as a support for the CuO–ZnO–ZrO_2–Al_2O_3/rGO catalyst to form methanol via CO_2 hydrogenation. In this case, the surface area of the CuO–ZnO–ZrO_2–Al_2O_3/reduced GR was 125.6 $m^2\ g^{-1}$. Moreover, the analysis showed that the use of rGO led to a growth of the adsorption capacity of CO_2 and H_2, with a CO_2 conversion of 14.7% at 513 K, 20 bar, and 6,075 h^{-1} space velocity. On the other hand, the methanol performance was 11.6%, higher compared with CuO–ZnO–ZrO_2–Al_2O_3/reduced GR without rGO (9.8%) (Fan and Wu, 2016).

In comparison to conventional thermal catalysis, which requires elevated pressures and temperatures, electrochemical reduction can occur at room temperature. This makes electrochemical reduction more attractive from an economic and environmental viewpoint. Zhang et al. investigated the use of tin oxide nanocrystals on GR supports as CO_2 reduction electrocatalysts. At 340 mV, a CO_2 reduction was observed to occur selectively. The highest Faradaic efficiencies for formate production are greater than 93% when $NaHCO_3$ solutions are used. The observed reactivity toward CO_2 reduction can be attributed to the compromise that occurs as a result of the interaction of $CO_2^{\bullet-}$ and the nanoscale tin surface, as well as to the kinetic activation toward protonation and further reduction (Zhang et al., 2014). Hussain et al. reported the formation of a nanocomposite composed of copper nanoparticles and rGO on a copper substrate. The obtained nanocomposite was optimized considering the composition of rGO and Cu, the analysis indicating that CO_2 could be reduced with a FE = 76.6% at −0.4 V. These noteworthy results indicated that this Cu-rGO nanocomposite has a promising potential when applied for CO_2 electrochemical reduction (Hossain et al., 2017). Geioushy et al. synthesized a GR/Cu_2O catalyst coated on Cu foil (Geioushy et al., 2017). The resulting GR/Cu_2O electrode (density of ~12.2 mA cm^{-2}) has a higher CO_2 reduction effect than the Cu_2O electrode (current ~8.4 mA cm^{-2}). The gas chromatography-mass spectrometry analysis indicated that the predominant product ethanol (~0.34 ppm) with a Faradaic efficiency of up to 9.93%.

GR-based catalysts can also be used in combination with solar energy to perform photocatalytic CO_2 reduction and to convert greenhouse gases into CH_4 and methanol (CH_3OH). Madhusudan et al. synthesized a hierarchical GR-$Zn_{0.5}Cd_{0.5}S$ nanocomposite with enhanced photocatalytic activity in the visible range. Compared to pure $Zn_{0.5}Cd_{0.5}S$ nanospheres, the 2 GR-ZCS (2 wt% GR-$Zn_{0.5}Cd_{0.5}S$) composite produced 98 times more CH_3OH (~1.96 μmol $g^{-1}\ h^{-1}$). These good results for photocatalytic CO_2 reduction can be explained by the presence of GR, which is a very good electron receiver and carrier (Madhusudan et al., 2020). Hiragond et al. (2021) synthetised a reduced Ti composite enfolded in N-doped GO for photocatalytic CO_2 reduction into CH_4 (Fig. 4). A small amount of Pt nanoparticles was deposited on the catalyst to improve the performance of the obtained N-doped GO, enfold

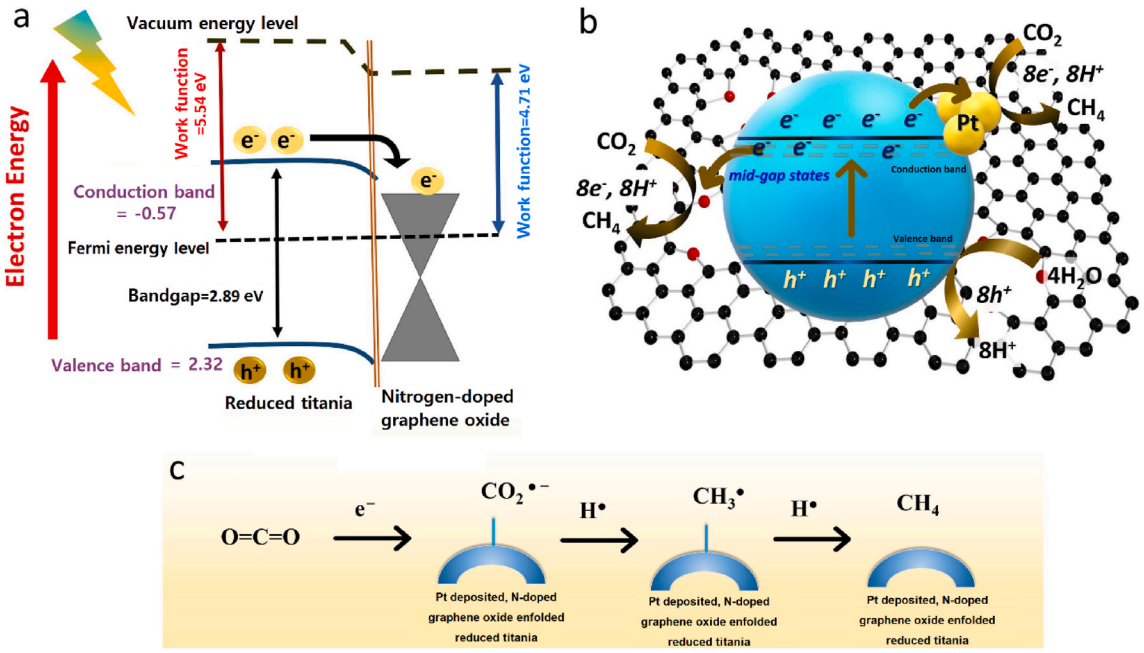

Fig. 4. (a) Energy band diagram of reduced titania enfolded with N-doped GO, (b) CO_2 reduction mechanism on Pt-deposited, N-doped GO enfolded reduced titania, and (c) photocatalytic CO_2 reduction to CH_4 on the catalyst surface, Modified and adapted by permission from Ref. (Hiragond et al., 2021) (#ID: 1204705).

reduced Ti and increased CH_4 formation. The result in Pt 1.0%-NGO-RT had a selective visible-light CO_2 reduction into CH_4 approximately 12 times better than pristine reduced titania and approximately 2 times than N-doped GO enfolded reduced Ti. The catalyst's analysis revealed that it is stable over 35 h. The electron transfer process was used to validate the photo-induced CO_2 reduction mechanism, as shown in Fig. 4. Under the solar-light illumination, the electrons in the valence band (VB) get excited and move to the conduction band (CB) of reduced titania, creating holes at VB. The created holes oxidize the water molecule to H_2, which further dissociates to form an $H^{\bullet}$ radical. Meanwhile, the photogenerated electrons transfer to the surface N-doped GO/Pt by interfacial charge transfer process and react with adsorbed CO_2 molecule, producing $CO_2^{\bullet -}$, which then reacts with $H^{\bullet}$ radical, generating $CH_3^{\bullet}$. Finally, CH_4 is formed by the reaction between $CH_3^{\bullet}$ and another $H^{\bullet}$ (Hiragond et al., 2021).

This was shown that Ni@graphitic carbon magnetic hollow spheres containing Ni nanoparticles encircled by graphitic carbon with only a few layers had a highly efficient photocatalytic CO_2 reduction. These spheres were obtained through a thermal annealing procedure applied to a Ni-containing metal-organic framework in a nitrogen atmosphere. The characterisation showed that the synthetised Ni@graphitic carbon spheres have a large surface area and a highly porous structure. In combination with a ruthenium photosensitiser and visible light irradiation, this catalyst has a CO production rate of 9.0 mmol h^{-1} g^{-1}. The analysis of the Ni@graphitic carbon photocatalyst showed that it is highly stable and can be reused by applying magnetic separation (Lin et al., 2019).

Another type of application for GR-based catalysts is represented by the CO_2 photo-electro-catalytic reduction. The photo-electro-catalytic CO_2 reduction under visible light was enhanced by Rezaul Karim et al., which used GO incorporated with copper ferrite ($CuFe_2O_4$). The characterisation study revealed a strong interaction between GO and $CuFe_2O_4$ in the hybrid catalyst. By including GO in the catalyst composition, photoexcited electrons from $CuFe_2O_4$ were trapped, resulting in a decrease in electrons/hole recombination. This resulted in a 28.8 mol L^{-1} cm^{-2} methanol performance at a quantum efficiency of 20.5%. Methanol had an incident photon current efficiency of 8.02% and a free electron efficiency of 87%. This data indicates that the photo-electro-catalytic activity applied to CO_2 reduction can be ameliorated using GO and $CuFe_2O_4$. Moreover, the team proposed a universal platform to fabricate GO – $CuFe_2O_4$ photocatalysts (Rezaul Karim et al., 2019).

To form a photo-electro-catalytic reactor for CO_2 conversion, Cheng et al. combined Pt- and Pt-modified TiO_2 nanotubes catalysts. CO_2 reduction was performed using a biased voltage and bandgap illumination. The proposed system had a combined liquid product generation rate for CH_3OH, C_2H_5OH, HCOOH, and CH_3COOH of ~600 nmol h^{-1} cm^{-2} and a carbon atom conversion rate of 1,130 nmol h^{-1} cm^{-2}. This conversion rate is significantly higher compared with those achieved using Pt and rGO separately (Cheng et al., 2014).

Although significant progress has been made in the application of GR for CO_2 reduction, several issues must be resolved before GR-based catalysts can be used on a large scale. Some of these issues focus on identifying the distinct function of the GR in the reaction, determining the case of poor stability in some applications, and improving general low activity (Pan et al., 2020). Table 3 summarises the GR-based catalysts for CO_2 reduction.

4.2. *Water treatment: Way towards cleaner production*

In the context of population rapid growth and dwindling clean water resources, the development of new materials that can be used in refining the strategies for raising the quality of water sources and drinking water is of utmost importance. In this context, graphene-based nanomaterials were extensively studied, these materials proving to have the potential to generate new ground-breaking techniques (He et al., 2018). In this section, the recent evolution of GR in composites used as catalysts in various applications of photocatalysis, advanced oxidation processes, and photo-electro-catalysis for wastewater treatment is analyzed.

For example, a dual application power generation and wastewater treatment developed by Li et al. employed a GO hybridized magnesium oxide (GO/magnesium oxide) nanocomposite to a cathode carbon cloth in a microbial fuel cell. In the GO/magnesium oxide composite, the magnesium oxide decorated the surface of GO. An analysis of the system represented that the electrochemical activity of GO/Magnesium oxide cathode was higher compared to a plain Magnesium oxide cathode or pure GO cathode. As a result, the power density of the proposed system was 755.63 mW m^{-2}, a value that represents 86.78% of the power

Table 3
GR-based catalysts for CO_2 reduction.

Catalyst type	Type of reduction process	Temperature (K)	Pressure (bar)	Electrolyte	CO_2 conversion (%)	Product/yield (μmol g^{-1} h^{-1})	Ref.
CuO–ZnO–ZrO_2–Al_2O_3/rGO	Electrochemical	513	20	1 M NaOH	14.7	Methanol/9700	Fan and Wu (2016)
Cu- rGO	Electrochemical	293.15	1	0.1 M $NaHCO_3$	69.2–76.6 (for various electrode)	Methane/-	Hossain et al. (2017)
GR/Cu_2O	Electrochemical	473.15	1	0.5 M $NaHCO_3$	Significant	Ethanol/-	Geioushy et al. (2017)
Ag_2/GR	Electrochemical	298.15		0.5 M $KHCO_3$	93.4	Carbon monoxide/-	Li et al. (2020)
GR -ZCS nanosphere	Photocatalytic	298.15	1	0.5 M Na_2SO_4	-	Methanol/1.96	Madhusudan et al. (2020)
Pt- Nitrogen-doped GO -RT	Photocatalytic	298.15	1	No sacrificial agents	-	Methane/0.252	Hiragond et al. (2021)
Ni@graphitic carbon	Photocatalytic	298.15	1	-	-	Carbon monoxide/9000	Lin et al. (2019)
TiO_2-Graphene	Photocatalytic	369.15	1	$NaHCO_3$ + H_2SO_4	95.3	Methane/26.7	Xu et al. (2019)
Nitrogen-based GR/CdS	Photocatalytic	298.15	1	-	-	Methane/0.33	Bie et al. (2019)
Ag_2Se-GR-TiO_2	Photocatalytic	298.15	1	H_2O containing $NsHCO_3$	-	Methanol/3.52	Ali and Oh (2017b)
PbSe-GR-TiO_2	Photocatalytic	298.15	1	Na_2SO_3/Na_2S	-	Methanol/4.35	Ali and Oh (2017a)
Cu- GO–TiO_2	Photocatalytic	298.15	1	250 mL sodium carbonate/bicarbonate buffer solution	-	Methanol/47	Pastrana-Martínez et al. (2016)
GR oxide/$CuFe_2O_4$	Photoelectrocatalytic	298.15	1	0.1 M $NaHCO_3$	-	Methanol/28.8	(Rezaul Rezaul Karim et al., 2019)
GR-TiO_2	Photoelectrocatalytic	298.15	1	0.1 M Na_2SO_4	-	Ethanol/-	Hasan et al. (2015b)
Cu- rGO–TiO_2	Photoelectrocatalytic	298.15	1	0.1 M Na_2SO_4	-	Methanol/255	Hasan et al. (2015a)

density of microbial fuel cells catalyzed with Pt/C. Moreover, the removal efficiency of chemical oxygen demand when using GO/Magnesium oxide was 79.5%, and the coulombic efficiency was 31.6%. Among the three cathodes tested, these values represent the best result. The power density of the system using the GO/Magnesium oxide cathode was at a stable level even after 20 cycles running. In addition, a reduction in the cost of 93.3% was achieved in comparison with the Pt/C catalyst (Li et al., 2017).

To produce GO/Mn_3O_4 (GO/Mn_3O_4) composites, Li et al. (2015) elaborated a very effective one-step method. This is based on a GO/$MnSO_4$ suspension obtained through an altered Hummer's method. In combination with air and KOH, the GO/$MnSO_4$ is converted *in situ* into a GO/Mn_3O_4 hybrid. This approach has one by-product, K_2SO_4 crystals, and it can be used as a green method. Tests of this hybrid on methylene blue decomposition showed that it has superior catalytic activities. At room temperature, tests show the reaction rate is improved compared to that of the bare Mn_3O_4 particles, resulting in 100% decolourised and 77% mineralised for 50 mL of methylene blue (50 mg L^{-1}) when 10 mg of GO/Mn_3O_4 is used. The synergistic effects of Mn_3O_4, H_2O_2, GO, and methylene blue molecules can account for these results. For methylene blue degradation, the catalytic activity of GO/Mn_3O_4 is influenced by the quantity of the $^{\bullet}OH$ species produced from H_2O_2 (Li et al., 2015).

In a study focusing on the degradation of organic contaminants through photo-Fenton processes, GO–Fe_2O_3 was employed as a heterogeneous catalyst. The combination of Fe_2O_3 and GO sheets was determined to be the consequence of metal–carbonyl coordination. To test the GO–Fe_2O_3 catalytic activity, the degradation of Rhodamine B and 4-nitrophenol (4NP) under visible light (>420 nm) in the presence of H_2O_2 was used as a case study. It was proved that an excellent catalytic property can be obtained for a pH ranging from 2.09 to 10.09 and that the system was stable after seven recycles. These results are explained by GO's adsorptive properties and the $^{\bullet}OH$ radicals produced during the heterogeneous photo-Fenton process. Thus, it has been demonstrated that GO–Fe_2O_3 is an effective catalyst for the degradation of organic pollutants (Guo et al., 2013). Another example focusing on Rhodamine B degradation is the work of Shao et al., who used a graphitic carbon nitride/rGO/ZnS composite in conjunction with visible irradiation. The results have shown that compared with the control group (carbon nitride/rGO, carbon nitride/ZS, and rGO/ZS), the proposed composite had a higher photocatalytic activity (about 97% after 60 min). This higher performance can be explained by the efficient charge separation, multistep transfer between rGO and carbon nitride/ZS, and improved absorption of visible light (Shao et al., 2016).

For wastewater treatment, Du et al. (2016) used a hybrid catalyst with long-term stability and high efficiency: heterogeneous manganese/magnetite/GO. When potassium peroxymonosulfate was activated, the catalyst generated sulfate radicals that removed bisphenol A from the water. The generation of hydroxyl radicals and sulfate radicals has been verified. The activation of potassium peroxymonosulfate in the considered system occurred as a result of electron transfer from MnO or Mn_2O_3 to potassium peroxymonosulfate, generating sulfate radicals, protons, and MnO_2. The GO has the role of immobilising the composite, providing a higher rate and better dispersibility of particle distribution (Du et al., 2016). The same pollutant was the focus of the Yang et al. (2016) work, where a TiO_2/graphene/Cu_2O mesh was applied under visible light. The mesh was synthesised by combining GR chemical vapour deposition and Cu_2O electrochemical vapour deposition. The high photocatalytic activity was observed by interconnected 3-dimensional channels within the TiO_2/GR/Cu_2O mesh (Yang et al., 2016).

The GR-based catalysts were also used for the degradation of wastewater, with an emphasis on organic pollutants. For example, Ai et al. (2015) investigated the photodegradation of methylene blue and C_6H_5OH using graphitic carbon nitride and rGO composites under various light irradiation conditions. The results indicated that the addition of GR promoted visible-light-induced methylene blue photodegradation. Additionally, a high rate of degradation of C_6H_5OH solutions was achieved (Ai et al., 2015).

When applying a GR-based catalyst for water treatment, one challenging aspect is represented by the active sites stripping as a result of the liquid environment. Another fact that should be considered is that the catalysts has to be recycled from the liquid. Table 4 summarises the GR-based catalysts for the degradation of pollutants.

Table 4
GR-based catalysts for the degradation of pollutants from water and wastewater.

Catalyst type	Type of process	Pollutants	Efficiency (%)	Cycling stability (%)	Ref.
rGO/SnO_2	Photocatalyst	Rhodamine B	98	96 (5 runs)	Shyamala and Devi (2020)
rGO/$BiVO_4$/ZnO	Photocatalyst	Ciprofloxacin	98.4	88 (6 runs)	Raja et al. (2020)
SAG-FeOOH/GO	Fenton-like reaction	Methylene blue	100	~100 (4 runs)	Sarkar and Yun (2021)
rGO/Fe_3O_4	Fenton-like reaction	Acid Green 25	100	-	Sadegh et al. (2021)
CoS-rGO	Peroxymonosulfate	Rhodamine B	100	~100 (8 runs)	Amirache et al. (2021)
GO/MgO	Microbial fuel cell	Chemical oxygen demand	79.5	-	Li et al. (2017)
GO/$MnSO_4$	Radical activation	Methylene blue	100	99.6 (4 runs)	Li et al. (2015)
GO–Fe_2O_3	Photo-Fenton	Rhodamine B	99	99 (7 runs)	Guo et al. (2013)
		4-Nitrophenol	92	-	
Manganese/magnetite/GO	Peroxymonosulfate	Bisphenol A	98	86 (5 runs)	Du et al. (2016)
g-C_3N_4/rGO/ZnS	Photocatalyst	Rhodamine B	97	62 (4 runs)	Shao et al. (2016)
g-C_3N_4/rGO	Photocatalyst	Methylene blue	100	-	Ai et al. (2015)
TiO_2/GR/Cu_2O	Photocatalyst	Bisphenol A	92	81 (5 runs)	Yang et al. (2016)
rGO/polyethyleneimine/Ag	Photocatalyst	Rhodamine B	100	-	Jiao et al. (2015)
$ZnFe_2O_4$–GR	Photocatalyst	Methylene blue	99	95 (10 runs)	Fu and Wang (2011)
Co_3O_4/GR	Peroxymonosulfate	Orange II	100	~100 (3 runs)	Wang et al. (2016)
Fe_3O_4–Mn_3O_4/rGO	Fenton-like	Sulfamethazine	98	-	Wan and Wang (2017)
Fe/Fe_3C@Fe/N-doped GR	Fenton	Rhodamine 6G	96	96 (13 runs)	Huang et al. (2017)
Nitrogen-doped GR aerogels	Peroxymonosulfate	Ibuprofen	92.6	28.4 (3 runs)	Wang et al. (2019)
GO–$FePO_4$	Photo-Fenton	Rhodamine B	97	95 (6 runs)	Guo et al. (2015)
Co_3O_4/GO	Sulfate radicals	Orange II	100	100 (5 runs)	Shi et al. (2012)
α-Fe_2O_3@GO	Photo-Fenton	Methylene blue	100	-	Liu et al. (2017)
Nitrogen-based GR	Electrochemical oxidation	Phenol	95.7	95 (5 runs)	Su et al. (2019)
Iron sludge-GR	Fenton	Rhodamine B	99	75.1 (5 runs)	Guo et al. (2017)
		Acid Red G	98.5	-	
		Metronidazole	91.8	-	

4.3. Air purification

Due to their impact on human health, volatile organic compounds degradation and NO_x abatement are aspects that deserve particular attention. As a result, various catalysts were studied concerning these types of reactions. In the context of GR development, a new direction in this area of research was established. One such example of studies is represented by the work of Bo et al. (2020) where a system using solar irradiation and post-plasma catalysis was proposed. Further, it was applied for toluene oxidation over a bi-functional GR fin foam decorated with a MnO_2 nanofins catalyst. An extensive analysis of this catalyst behaviour indicated that it could achieve a high rate of capturing and converting the solar energy into heat, with an absorption rate higher than 95%. This effectiveness allowed a temperature increase of the catalyst bed to 55.6 °C at 1 sun irradiation and light intensity of 1,000 W m^{-2}. Compared with the quantity of catalyst used in previous works (which usually varies from 100 to 1,000 mg), in the proposed post-plasma catalysis-MnO_2/bifunctional GR fin foam, the catalyst weight used in this identified study was from 10 to 100 times lower (9.8 mg). The use of solar thermal conversion increased the C_7H_8 conversion and CO_2 selectivity by 36–63%. 93% efficiency was reached for C_7H_8 conversion and 83% for CO_2 selectivity. These remarkable results were obtained using specific input energy of approximately 350 J L^{-1}, implying a significant reduction in the energy consumption of the plasma-catalytic gas cleaning system. The energy efficiency of C_7H_8 conversion using the solar-based post-plasma catalytic procedure is up to 12.7 g kWh^{-1}, which is approximately 57% higher than the energy efficiency of post-plasma catalysis without solar irradiation (8.1 g kWh^{-1}). At the same time, the energy utilisation of the solar-enhanced post-plasma catalytic is lowered by 35–52% compared with the post-plasma catalysis process. Additionally, the solar irradiation-induced excellent self-cleaning capability for MnO_2/bifunctional GR fin foam, which has long-term catalytic stability of 72 h at 1 sun. The combined effect of solar irradiation and post-plasma catalysis process can be explained by: i) the solar-induced thermal effect on the catalyst bed; ii) the improved ozone decomposition (that was ~3 times higher for solar-based post-plasma catalytic procedure ~0.52 g_{O3} g^{-1} h^{-1} compared with ~0.18 g_{O3} g^{-1} h^{-1} for post-plasma catalysis); this resulted in the generation of more oxidative species and the enhancement the catalytic oxidation; and iii) the capacity of the catalyst to self-clean at the high temperatures generated by solar irradiation (Bo et al., 2020). The mechanism describing this system is shown in Fig. 5.

Hu et al. (2014) proposed a new procedure for the fabrication of GR composites with varying MnO_2 loadings. The procedure is based on a direct redox reaction between GO and $KMnO_4$ at a temperature of 160 °C for 12 h in a hydrothermal environment. Numerous analyses have demonstrated that the proposed strategy is effective at producing tightly bound birnessite-type MnO_2 on GR. MnO_2 nanoparticles were distributed uniformly on the GR nanosheets in the obtained samples, with a MnO_2 loading of 64.6 wt % at room temperature (22 °C), the behaviour of GR, MnO_2, and the MnO_2/GR composite was analysed for catalytic ozonation of C_7H_8. The observations indicated that the amount of MnO_2 loaded onto GR affected the catalytic activity, with the highest C_7H_8 decomposition rate of 7.89 × 10^{-6} mol min^{-1} g^{-1} obtained for a MnO_2/GR ratio of 64.6 wt %. This is explained by the strong correlation between the active sites on GR responsible for toluene adsorption and ozone decomposition and the MnO_2 on GR responsible for ozone decomposition (Hu et al., 2014).

In another work focusing on photocatalytic NO_x oxidation under visible light and UV conditions, a material combining TiO_2 with surfactant-stabilised GR and rGO was utilized (Trapalis et al., 2016). In comparison to pure TiO_2, the proposed composite demonstrated superior performance, with the difference being most pronounced when exposed to visible light. A detailed analysis of various cases of TiO_2/-surfactant-stabilised GR, TiO_2/rGO and TiO_2/(surfactant-stabilised GR and rGO) indicated that the photocatalytic performance for NO_x removal follows two trends. First, for TiO_2/surfactant-stabilised GR and TiO_2/rGO, the efficiency was, to some extent, enhanced under UV light. This is due to the interaction between TiO_2 and GR and the fact that the GR sheets are electron traps for surfactant-stabilised GR and photosensitizers for rGO. Second, for TiO_2/(surfactant-stabilised GR and rGO), low NO_2 release was attained (Keshmiri et al., 2021).

A detailed analysis of the mechanisms and behaviour resulting from the addition of GR to catalysts for air decontamination indicates the following:

(i) Charge recombination is inhibited by electron transfer from a catalytically active species to GR

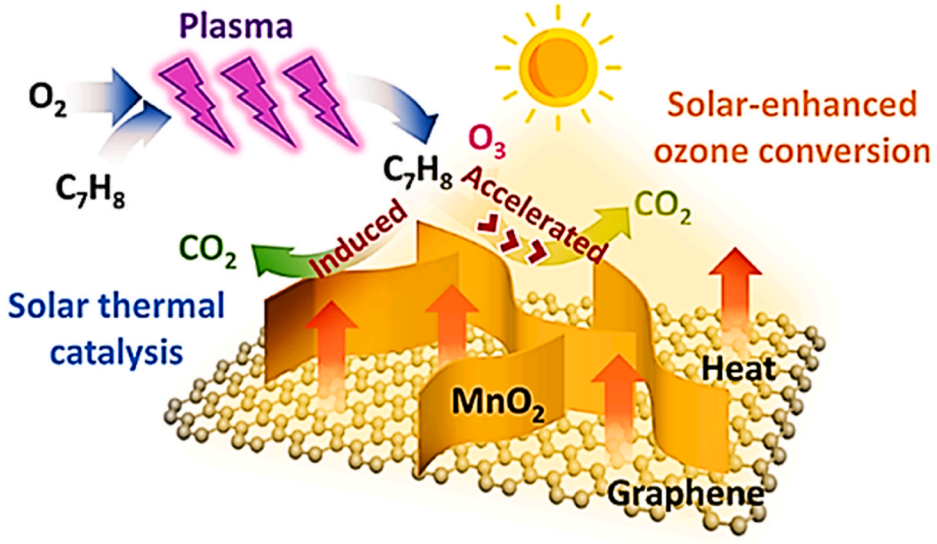

Fig. 5. A mechanism for solar-enhanced plasma-catalytic oxidation of toluene over nanofin-like MnO_2/bifunctional GR fin foam, Copyright (2020)American Chemical Society (Bo et al., 2020) (#ID: CSCSI0024848).

(ii) The formation of new chemical bonds causes a reduction in the bandgap of the catalytically active species and a broadening of the photoresponse range
(iii) The interaction between the aromatic regions of GR and the target molecules enhances the pollutant's adsorption on the catalyst, and
(iv) The facilitating effect of GR on charge transfer is limited.

5. Outlooks

Although still at a very early stage, advancements in the application, characterisation, and synthesis of nanomaterials containing GR as one of the main framework's concepts of cleaner production toward environmental sustainability are discussed in this review. Notwithstanding the considerable efforts invested in this sphere of research, several issues should be resolved before broad applicability is achieved. These issues include unclear mechanisms and/or lack of a basic understanding of the function of GR; complex problems related to the preparation of GR and its derivates on a large scale; and finite stability in specific reactions (e.g., photocatalysis). Consequently, further advancements in specific research directions are needed to fully exploit the extraordinary potential possessed by GR-based nanomaterials.

The first research direction concerns the development of new synthetic methods for producing large quantities of high-quality GR nanomaterials. Until now, the focus has been on only two methods: graphite oxide exfoliation and chemical vapour deposition. However, alternatives that can reduce manufacturing costs, enable precise manipulation of doping (amount and type), and upgrade catalytic efficiency are required. As composites containing GR and conventional catalysts or supports can have somewhat surprising properties, research on these compounds could yield new avenues for development.

As the first research direction focuses on the economic aspects of large-scale production, another important aspect of production is strategies for controlling the characteristics of the nanomaterials produced. Most GR and its derivatives are produced via chemical exfoliation. However, this method results in the production of GR sheets with low electrical conductivity. In this context, approaches for synthesizing conductive GR materials with configurable nanostructures are required for the development of high-performance electro- and photo-catalysts which can lead to the cleaner production to move towards a circular and sustainable economy.

The third direction involves combining theoretical computations and experimental observations to gain a complete picture of the compounds' roles in GR-based nanomaterials, as well as their structure. This combined strategy enables the investigation of the interactions between GR and loaded catalyst species, the types of doping sites that are more active than others, the amount of activation energy required, and the progression of initial reaction pathways.

The fourth direction revolves around the production of composite catalysts with controllable sizes and uniform morphologies. Using conventional approaches, this is largely unachievable because of the limitations of the methods currently used to synthesise processible GR-based composites. These methods and the assembly mechanisms of GR-based composite sheets and other functional components require further study. The other research direction in which additional research and advancements can be achieved pertains to the catalysation mechanisms of GR catalysts. This is because these aspects are only partially known, and some of the current explanations are not widely accepted.

Finally, another identified research direction is research on a metal-free GR-based catalyst. Some researchers have expressed reservations about this type of catalyst. However, this can also represent areas of research on supportable catalysis. Considering that most existing studies focus on photocatalytic and electrochemical processes, additional reaction types should be explored for their potential application as one of the emerging methods and technologies for cleaner production and prevention of environmental damage.

6. Conclusions

Cleaner production as a continuously emerging and efficient strategy makes a significant contribution to preventing environmental pollution as well as improving production towards a circular and sustainable economy. The cleaner production approach can reduce the environmental impact of rapid industrial development and the resulting hazards to the ecosystem. During the past decade, GR remains a unique material endowed with properties that allow for wide application in electronics, sensors, energy harvesting and storage, membranes, multifunctional composites and coatings, biotechnology, medicine, etc. The unique properties of GR, such as high surface area, charge transfer, and adsorption capability, have opened great possibilities to enhance the efficiency of numerous environmental processes. Besides, GR composites made up of GR derivatives with conventional materials could significantly improve the effectiveness of catalysis by extending the light absorption ability and photostability, as well as enhancing pollutant

adsorption, catalysis etc., and making them attractive for environmental applications. This review summarises the most significant applications of GR materials in the development of a variety of novel catalysts as aspects of a cleaner production strategy. The intrinsic catalytic properties of GR-based nanomaterials and the performance enhancements that these materials induce in other catalysts when combined to form functional composites enable the development of highly beneficial solutions for a wide variety of cleaner production applications. The superior properties of GR-based catalysts are primarily due to the GR sheets' atomic-thick two-dimensional structure, functional groups, large specific surface area, and electrical properties. This study covers preparation, characterisation, and applications, with a focus on pollutant degradation, CO_2 reduction, and air purification. In each case, the challenges of the reactions under study are analysed and discussed. It is clearly shown that GR-based nanomaterials are the basis for future catalysts for cleaner production. This is largely due to the characteristics of GR-based nanomaterials, which include their ease of modification, their large specific surface area, their high thermal and electrical conductivity, their high adsorption capacity, their high mechanical strength, and their eco-friendliness. All of these properties make it possible to design and develop a variety of novel GR-based catalysts with increased efficiency.

Declaration of competing interest

The authors declare that they have no known competing financial interests or personal relationships that could have appeared to influence the work reported in this paper.

Acknowledgements

SWJ and YV would like to acknowledge the financial support from the Korea Environment Industry & Technology Institute (KEITI) through the Technology Development Project for Safety Management of Household Chemical Product Program, funded by the Korea Ministry of Environment (MOE) (2020002970005, 1485017845). Also, the EU supported project Sustainable Process Integration Laboratory – SPIL funded as project No. CZ.02.1.01/0.0/0.0/15_003/0000456, by Czech Republic Operational Programme Research and Development, Education, Priority 1: Strengthening capacity for quality research under the collaboration agreement with Universiti Teknologi Malaysia, Johor Bahru has also been gratefully acknowledged. The authors also gratefully acknowledge support from the Universiti Teknologi Malaysia and Post-Doctoral fellow (Teaching & Learning) Scheme under MJIIT-UTM.

References

Agarwal, V., Zetterlund, P.B., 2020. Strategies for reduction of graphene oxide-A comprehensive review. Chem. Eng. J. 405, 127018.
Ai, B., Duan, X., Sun, H., Qiu, X., Wang, S., 2015. Metal-free graphene-carbon nitride hybrids for photodegradation of organic pollutants in water. Catal. Today 258, 668–675.
Akshatha, S., Sreenivasa, S., Kumar, K.Y., Archana, S., Prashanth, M., Prasanna, B., Chakraborty, P., Krishnaiah, P., Raghu, M., Alrobei, H., 2020. Rutile, mesoporous ruthenium oxide decorated graphene oxide as an efficient visible light driven photocatalyst for hydrogen evolution reaction and organic pollutant degradation. Mater. Sci. Semicond. Process. 116, 105156.
Ali, A., Oh, W.-C., 2017a. A simple ultrasono-synthetic route of PbSe-graphene-TiO2 ternary composites to improve the photocatalytic reduction of CO2. Fullerenes, Nanotub. Carbon Nanostruct. 25 (8), 449–458.
Ali, A., Oh, W.-C., 2017b. Synthesis of Ag2Se–graphene–TiO2 nanocomposite and analysis of photocatalytic activity of CO2 reduction to CH3OH. Bull. Mater. Sci. 40 (7), 1319–1328.
Amirache, L., Barka-Bouaifel, F., Borthakur, P., Das, M.R., Ahouari, H., Vezin, H., Barras, A., Ouddane, B., Szunerits, S., Boukherroub, R., 2021. Cobalt sulfide-reduced graphene oxide: an efficient catalyst for the degradation of rhodamine B and pentachlorophenol using peroxymonosulfate. J. Environ. Chem. Eng. 9 (5), 106018.
An, D., Yang, L., Wang, T.-J., Liu, B., 2016. Separation performance of graphene oxide membrane in aqueous solution. Ind. Eng. Chem. Res. 55(17), 4803-4810.
Bai, H., Li, C., Shi, G., 2011. Functional composite materials based on chemically converted graphene. Adv. Mater. 23 (9), 1089–1115.
Barra, A., Lazăr, O., Pantazi, A., Hortigüela, M.J., Otero-Irurueta, G., Enăchescu, M., Ruiz-Hitzky, E., Nunes, C., Ferreira, P., 2021. Joining Caffeic acid and hydrothermal treatment to produce environmentally benign highly reduced graphene oxide. Nanomaterials 11 (3), 732.
Bhushan, R., Kumar, P., Thakur, A., 2020. Catalyst-free solvothermal synthesis of ultrapure elemental N-and B-doped graphene for energy storage application. Solid State Ionics 353, 115371.
Bie, C., Zhu, B., Xu, F., Zhang, L., Yu, J., 2019. In situ grown monolayer N-doped graphene on CdS hollow spheres with seamless contact for photocatalytic CO_2 reduction. Adv. Mater. 31 (42), 1902868.
Bo, Z., Yang, S., Kong, J., Zhu, J., Wang, Y., Yang, H., Li, X., Yan, J., Cen, K., Tu, X., 2020. Solar-enhanced plasma-catalytic oxidation of toluene over a bifunctional graphene fin foam decorated with nanofin-like MnO_2. ACS Catal. 10 (7), 4420–4432.
Bond, G., Thompson, D., 1999. Gold catalysis. Catal. Rev. Sci. Eng. 41, 319–388.
Bu, Y., Liang, H., Gao, K., Zhang, B., Zhang, X., Shen, X., Li, H., Zhang, J., 2020. Wafer-scale fabrication of high-purity reduced graphene oxide films as ultrahigh-frequency capacitors with minimal self-discharge. Chem. Eng. J. 390, 124560.
Bundaleska, N., Henriques, J., Abrashev, M., Botelho do Rego, A., Ferraria, A., Almeida, A., Dias, F., Valcheva, E., Arnaudov, B., Upadhyay, K., 2018. Large-scale synthesis of free-standing N-doped graphene using microwave plasma. Sci. Rep. 8 (1), 1–11.
Buron, J.D., Pizzocchero, F., Jepsen, P.U., Petersen, D.H., Caridad, J.M., Jessen, B.S., Booth, T.J., Bøggild, P., 2015. Graphene mobility mapping. Sci. Rep. 5 (1), 1–7.
Cao, N., Luo, W., Cheng, G., 2013. One-step synthesis of graphene supported Ru nanoparticles as efficient catalysts for hydrolytic dehydrogenation of ammonia borane. Int. J. Hydrogen Energy 38 (27), 11964–11972.
Chen, D., Cheng, Y., Zhou, N., Chen, P., Wang, Y., Li, K., Huo, S., Cheng, P., Peng, P., Zhang, R., 2020. Photocatalytic degradation of organic pollutants using TiO_2-based photocatalysts: a review. J. Clean. Prod. 268, 121725.
Chen, P., Xiao, T.-Y., Li, H.-H., Yang, J.-J., Wang, Z., Yao, H.-B., Yu, S.-H., 2012. Nitrogen-doped graphene/ZnSe nanocomposites: hydrothermal synthesis and their enhanced electrochemical and photocatalytic activities. ACS Nano 6 (1), 712–719.
Chen, Y., Wu, H., Duan, R., Zhang, K., Meng, W., Li, Y., Qu, H., 2022. Graphene doped Sn flame retardant prepared by ball milling and synergistic with hexaphenoxy cyclotriphosphazene for epoxy resin. J. Mater. Res. Technol. 17, 774–788.
Chen, Y., Zhang, X., Zhang, D., Yu, P., Ma, Y., 2011. High performance supercapacitors based on reduced graphene oxide in aqueous and ionic liquid electrolytes. Carbon 49 (2), 573–580.
Cheng, J., Zhang, M., Wu, G., Wang, X., Zhou, J., Cen, K., 2014. Photoelectrocatalytic reduction of CO_2 into chemicals using Pt-modified reduced graphene oxide combined with Pt-modified TiO_2 nanotubes. Environ. Sci. Technol. 48 (12), 7076–7084.
Cherian, A.R., Benny, L., George, A., Varghese, A., Hegde, G., 2021. Recent advances in functionalization of carbon nanosurface structures for electrochemical sensing applications: tuning and turning. J. Nanostruct. Chem. https://doi.org/10.1007/s40097-021-00426-5.
Chua, C.K., Pumera, M., 2013. Reduction of graphene oxide with substituted borohydrides. J. Mater. Chem. 1 (5), 1892–1898.
Chua, C.K., Sofer, Z., Khezri, B., Webster, R.D., Pumera, M., 2016. Ball-milled sulfur-doped graphene materials contain metallic impurities originating from ball-milling apparatus: their influence on the catalytic properties. Phys. Chem. Chem. Phys. 18 (27), 17875–17880.
Dan, M., Vulcu, A., Porav, S.A., Leostean, C., Borodi, G., Cadar, O., Berghian-Grosan, C., 2021. Eco-friendly nitrogen-doped graphene preparation and design for the oxygen reduction reaction. Molecules 26 (13), 3858.
De Silva, K.K.H., Huang, H.-H., Yoshimura, M., 2018. Progress of reduction of graphene oxide by ascorbic acid. Appl. Surf. Sci. 447, 338–346.
Deokar, G., Jin, J., Schwingenschlögl, U., Costa, P.M.F.J., 2022. Chemical vapor deposition-grown nitrogen-doped graphene's synthesis, characterization and applications. npj 2D Mater. Appl. 6 (1), 14. https://doi.org/10.1038/s41699-022-00287-8.
Ding, Y., Zhu, X., Xiao, S., Hu, H., Frandsen, L.H., Mortensen, N.A., Yvind, K., 2015. Effective electro-optical modulation with high extinction ratio by a graphene–silicon microring resonator. Nano Lett. 15 (7), 4393–4400.
Dreyer, D.R., Bielawski, C.W., 2011. Carbocatalysis: heterogeneous carbons finding utility in synthetic chemistry. Chem. Sci. 2 (7), 1233–1240.
Du, J., Bao, J., Liu, Y., Ling, H., Zheng, H., Kim, S.H., Dionysiou, D.D., 2016. Efficient activation of peroxymonosulfate by magnetic Mn-MGO for degradation of bisphenol A. J. Hazard Mater. 320, 150–159.
El-Kady, M.F., Strong, V., Dubin, S., Kaner, R.B., 2012. Laser scribing of high-performance and flexible graphene-based electrochemical capacitors. Science 335 (6074), 1326–1330.
Fadil, Y., Thickett, S.C., Agarwal, V., Zetterlund, P.B., 2022. Synthesis of graphene-based polymeric nanocomposites using emulsion techniques. Prog. Polym. Sci. 125, 101476.
Fan, X., Peng, W., Li, Y., Li, X., Wang, S., Zhang, G., Zhang, F., 2008. Deoxygenation of exfoliated graphite oxide under alkaline conditions: a green route to graphene preparation. Adv. Mater. 20 (23), 4490–4493.
Fan, Y.J., Wu, S.F., 2016. A graphene-supported copper-based catalyst for the hydrogenation of carbon dioxide to form methanol. J. CO2 Util. 16, 150–156.
Fu, Y., Wang, X., 2011. Magnetically separable ZnFe2O4–graphene catalyst and its high photocatalytic performance under visible light irradiation. Ind. Eng. Chem. Res. 50 (12), 7210–7218.
Gayathri, S., Arunkumar, P., Kim, E.J., Kim, S., Kang, I., Han, J.H., 2019. Mesoporous nitrogen-doped carbon@ graphene nanosheets as ultra-stable anode for lithium-ion

batteries–Melamine as surface modifier than nitrogen source. Electrochim. Acta 318, 290–301.
Geioushy, R.A., Khaled, M.M., Hakeem, A.S., Alhooshani, K., Basheer, C., 2017. High efficiency graphene/Cu_2O electrode for the electrochemical reduction of carbon dioxide to ethanol. J. Electroanal. Chem. 785, 138–143.
Gnana Kumar, G., Kirubaharan, C.J., Udhayakumar, S., Karthikeyan, C., Nahm, K.S., 2014. Conductive polymer/graphene supported platinum nanoparticles as anode catalysts for the extended power generation of microbial fuel cells. Ind. Eng. Chem. Res. 53 (43), 16883–16893.
Guo, H., Li, Z., Xiang, L., Jiang, N., Zhang, Y., Wang, H., Li, J., 2021. Efficient removal of antibiotic thiamphenicol by pulsed discharge plasma coupled with complex catalysis using graphene-WO3-Fe3O4 nanocomposites. J. Hazard Mater. 403, 123673.
Guo, J., Zhang, S., Zheng, M., Tang, J., Liu, L., Chen, J., Wang, X., 2020. Graphitic-N-rich N-doped graphene as a high performance catalyst for oxygen reduction reaction in alkaline solution. Int. J. Hydrogen Energy 45 (56), 32402–32412.
Guo, S., Yuan, N., Zhang, G., Yu, J.C., 2017. Graphene modified iron sludge derived from homogeneous Fenton process as an efficient heterogeneous Fenton catalyst for degradation of organic pollutants. Microporous Mesoporous Mater. 238, 62–68.
Guo, S., Zhang, G., Guo, Y., Yu, J.C., 2013. Graphene oxide–Fe2O3 hybrid material as highly efficient heterogeneous catalyst for degradation of organic contaminants. Carbon 60, 437–444.
Guo, S., Zhang, G., Yu, J.C., 2015. Enhanced photo-Fenton degradation of rhodamine B using graphene oxide–amorphous $FePO_4$ as effective and stable heterogeneous catalyst. J. Colloid Interface Sci. 448, 460–466.
Hasan, M.R., Abd Hamid, S.B., Basirun, W.J., Meriam Suhaimy, S.H., Che Mat, A.N., 2015a. A sol–gel derived, copper-doped, titanium dioxide–reduced graphene oxide nanocomposite electrode for the photoelectrocatalytic reduction of CO2 to methanol and formic acid. RSC Adv. 5 (95), 77803–77813.
Hasan, M.R., Hamid, S.B.A., Basirun, W.J., 2015b. Charge transfer behavior of graphene-titania photoanode in CO2 photoelectrocatalysis process. Appl. Surf. Sci. 339, 22–27.
Hasani, A., Teklagne, M.A., Do, H.H., Hong, S.H., Van Le, Q., Ahn, S.H., Kim, S.Y., 2020. Graphene-based catalysts for electrochemical carbon dioxide reduction. Carbon Energy 2 (2), 158–175.
Hassani, S.S., Samiee, L., Ghasemy, E., Rashidi, A., Ganjali, M.R., Tasharrofi, S., 2018. Porous nitrogen-doped graphene prepared through pyrolysis of ammonium acetate as an efficient ORR nanocatalyst. Int. J. Hydrogen Energy 43 (33), 15941–15951.
He, K., Chen, G., Zeng, G., Chen, A., Huang, Z., Shi, J., Huang, T., Peng, M., Hu, L., 2018. Three-dimensional graphene supported catalysts for organic dyes degradation. Appl. Catal. B Environ. 228, 19–28.
Hiragond, C.B., Lee, J., Kim, H., Jung, J.-W., Cho, C.-H., In, S.-I., 2021. A novel N-doped graphene oxide enfolded reduced titania for highly stable and selective gas-phase photocatalytic CO_2 reduction into CH_4: an in-depth study on the interfacial charge transfer mechanism. Chem. Eng. J. 416, 127978.
Hossain, M.N., Wen, J., Chen, A., 2017. Unique copper and reduced graphene oxide nanocomposite toward the efficient electrochemical reduction of carbon dioxide. Sci. Rep. 7 (1), 3184.
Hu, C., Liu, D., Xiao, Y., Dai, L., 2018. Functionalization of graphene materials by heteroatom-doping for energy conversion and storage. Prog. Nat. Sci.: Mater. Int. 28 (2), 121–132.
Hu, M., Hui, K.S., Hui, K.N., 2014. Role of graphene in MnO_2/graphene composite for catalytic ozonation of gaseous toluene. Chem. Eng. J. 254, 237–244.
Hu, M., Yao, Z., Wang, X., 2017. Graphene-based nanomaterials for catalysis. Ind. Eng. Chem. Res. 56 (13), 3477–3502.
Hu, Y., Song, S., Lopez-Valdivieso, A., 2015. Effects of oxidation on the defect of reduced graphene oxides in graphene preparation. J. Colloid Interface Sci. 450, 68–73.
Huang, C., Li, C., Shi, G., 2012. Graphene based catalysts. Energy Environ. Sci. 5 (10), 8848–8868.
Huang, X., Niu, Y., Hu, W., 2017. Fe/Fe3C nanoparticles loaded on Fe/N-doped graphene as an efficient heterogeneous Fenton catalyst for degradation of organic pollutants. Colloids Surf. A Physicochem. Eng. Asp. 518, 145–150.
Huet, B., Raskin, J.-P., Snyder, D.W., Redwing, J.M., 2020. Fundamental limitations in transferred CVD graphene caused by Cu catalyst surface morphology. Carbon 163, 95–104.
Hussain, R.T., Islam, A.K.M.S., Khairuddean, M., Suah, F.B.M., 2022. A polypyrrole/GO/ZnO nanocomposite modified pencil graphite electrode for the determination of andrographolide in aqueous samples. Alex. Eng. J. 61 (6), 4209–4218.
Jakhar, R., Yap, J.E., Joshi, R., 2020. Microwave reduction of graphene oxide. Carbon 170, 277–293.
Jeon, W.-S., Kim, C.H., Wee, J.-H., Kim, J.H., Kim, Y.A., Yang, C.-M., 2021. Sulfur-doping effects on the supercapacitive behavior of porous spherical graphene electrode derived from layered double hydroxide template. Appl. Surf. Sci. 558, 149867.
Jiang, F., Zhang, J., Li, N., Liu, C., Zhou, Y., Yu, X., Sun, L., Song, Y., Zhang, S., Wang, Z., 2019. Nitrogen-doped graphene prepared by thermal annealing of fluorinated graphene oxide as supercapacitor electrode. J. Chem. Technol. Biotechnol. 94 (11), 3530–3537.
Jiang, N., Li, X., Guo, H., Li, J., Shang, K., Lu, N., Wu, Y., 2021. Plasma-assisted catalysis decomposition of BPA over graphene-CdS nanocomposites in pulsed gas-liquid hybrid discharge: photocorrosion inhibition and synergistic mechanism analysis. Chem. Eng. J. 412, 128627.
Jiao, T., Guo, H., Zhang, Q., Peng, Q., Tang, Y., Yan, X., Li, B., 2015. Reduced graphene oxide-based silver nanoparticle-containing composite hydrogel as highly efficient dye catalysts for wastewater treatment. Sci. Rep. 5 (1), 11873.
Jin, S., Yang, S.Y., Lee, J.M., Kang, M.S., Choi, S.M., Ahn, W., Fuku, X., Modibedi, R.M., Han, B., Seo, M.H., 2021. Fluorine-decorated graphene nanoribbons for an anticorrosive polymer electrolyte membrane fuel cell. ACS Appl. Mater. Interfaces 13 (23), 26936–26947.
Kang, J.H., Choi, S., Park, Y.J., Park, J.S., Cho, N.S., Cho, S., Walker, B., Choi, D.S., Shin, J.-W., Seo, J.H., 2021. Cu/graphene hybrid transparent conducting electrodes for organic photovoltaic devices. Carbon 171, 341–349.
Kanjwal, M.A., Lo, K.K.S., Leung, W.W.-F., 2019. Graphene composite nanofibers as a high-performance photocatalyst for environmental remediation. Separ. Purif. Technol. 215, 602–611.
Keramatinia, M., Ramezanzadeh, M., Bahlakeh, G., Ramezanzadeh, B., 2021. Synthesis of a multi-functional zinc-centered nitrogen-rich graphene-like thin film from natural sources on the steel surface for achieving superior anti-corrosion properties. Corrosion Sci. 178, 109077.
Keshmiri, N., Najmi, P., Ramezanzadeh, M., Ramezanzadeh, B., 2021. Designing an eco-friendly lanthanide-based metal organic framework (MOF) assembled graphene-oxide with superior active anti-corrosion performance in epoxy composite. J. Clean. Prod. 319, 128732.
KF, G.L.S.B.P., Andersson, R., 2017. Pourrahimi AM Strom V. Farris S. Olsson RT. Nanoscale 9, 9562–9571.
Kovtyukhova, N.I., Ollivier, P.J., Martin, B.R., Mallouk, T.E., Chizhik, S.A., Buzaneva, E. V., Gorchinskiy, A.D., 1999. Layer-by-layer assembly of ultrathin composite films from micron-sized graphite oxide sheets and polycations. Chem. Mater. 11 (3), 771–778.
Kumar, P., Shahzad, F., Yu, S., Hong, S.M., Kim, Y.-H., Koo, C.M., 2015. Large-area reduced graphene oxide thin film with excellent thermal conductivity and electromagnetic interference shielding effectiveness. Carbon 94, 494–500.
Kumar, R., Barakat, M., Taleb, M.A., Seliem, M.K., 2020. A recyclable multifunctional graphene oxide/SiO2@ polyaniline microspheres composite for Cu (II) and Cr (VI) decontamination from wastewater. J. Clean. Prod. 268, 122290.
Lambert, T.N., Chavez, C.A., Hernandez-Sanchez, B., Lu, P., Bell, N.S., Ambrosini, A., Friedman, T., Boyle, T.J., Wheeler, D.R., Huber, D.L., 2009. Synthesis and characterization of titania– graphene nanocomposites. J. Phys. Chem. C 113 (46), 19812–19823.
Le, V.T., Vasseghian, Y., Dragoi, E.-N., Moradi, M., Mousavi Khaneghah, A., 2021. A review on graphene-based electrochemical sensor for mycotoxins detection. Food Chem. Toxicol. 148, 111931.
Lee, S.P., Ali, G.A., Hegazy, H., Lim, H.N., Chong, K.F., 2021. Optimizing reduced graphene oxide aerogel for a supercapacitor. Energy Fuel. 35 (5), 4559–4569.
Li, B., Jin, X., Lin, J., Chen, Z., 2018. Green reduction of graphene oxide by sugarcane bagasse extract and its application for the removal of cadmium in aqueous solution. J. Clean. Prod. 189, 128–134.
Li, M., Zhou, S., Xu, M., 2017. Graphene oxide supported magnesium oxide as an efficient cathode catalyst for power generation and wastewater treatment in single chamber microbial fuel cells. Chem. Eng. J. 328, 106–116.
Li, N., Yue, Q., Gao, B., Xu, X., Su, R., Yu, B., 2019. One-step synthesis of peanut hull/graphene aerogel for highly efficient oil-water separation. J. Clean. Prod. 207, 764–771.
Li, X., Wang, H., Robinson, J.T., Sanchez, H., Diankov, G., Dai, H., 2009. Simultaneous nitrogen doping and reduction of graphene oxide. J. Am. Chem. Soc. 131 (43), 15939–15944.
Li, Y., Chen, C., Cao, R., Pan, Z., He, H., Zhou, K., 2020. Dual-atom Ag2/graphene catalyst for efficient electroreduction of CO2 to CO. Appl. Catal. B Environ. 268, 118747.
Li, Y., Chen, H., Voo, L.Y., Ji, J., Zhang, G., Zhang, G., Zhang, F., Fan, X., 2012. Synthesis of partially hydrogenated graphene and brominated graphene. J. Mater. Chem. 22 (30), 15021–15024.
Li, Y., Qu, J., Gao, F., Lv, S., Shi, L., He, C., Sun, J., 2015. In situ fabrication of Mn_3O_4 decorated graphene oxide as a synergistic catalyst for degradation of methylene blue. Appl. Catal. B Environ. 162, 268–274.
Lin, X., Wang, S., Tu, W., Wang, H., Hou, Y., Dai, W., Xu, R., 2019. Magnetic hollow spheres assembled from graphene-encapsulated nickel nanoparticles for efficient photocatalytic CO_2 reduction. ACS Appl. Energy Mater. 2 (10), 7670–7678.
Liu, L., Zhou, Z., Guo, Q., Yan, Z., Yao, Y., Goodman, D.W., 2011. The 2-D growth of gold on single-layer graphene/Ru (0001): enhancement of CO adsorption. Surf. Sci. 605 (17–18), L47–L50.
Liu, W., Speranza, G., 2021. Tuning the oxygen content of reduced graphene oxide and effects on its properties. ACS Omega 6 (9), 6195–6205.
Liu, Y., Jin, W., Zhao, Y., Zhang, G., Zhang, W., 2017. Enhanced catalytic degradation of methylene blue by α-Fe_2O_3/graphene oxide via heterogeneous photo-Fenton reactions. Appl. Catal. B Environ. 206, 642–652.
Liu, Y., Min, Z., Jiang, J., Sun, K., Gao, J., Shang, Y., Li, B., 2019. Molybdenum, cobalt sulfide-modified N-, S-doped graphene from low-temperature molecular pyrolysis: mutual activation effect for hydrogen evolution. ACS Sustain. Chem. Eng. 7 (24), 19442–19452.
Lopes, J.L., Martins, M.J., Nogueira, H.I.S., Estrada, A.C., Trindade, T., 2021. Carbon-based heterogeneous photocatalysts for water cleaning technologies: a review. Environ. Chem. Lett. 19 (1), 643–668.
Ma, B., Li, B., Li, Y., Fan, X., Zhang, F., Zhang, G., Zhu, Y., Peng, W., 2021. Synthesis of nitrogen and sulfur Co-doped carbon with special hollow sphere structure for enhanced catalytic oxidation. Separ. Purif. Technol. 278, 119522.
Ma, L., Zhang, J.-M., Xu, K.-W., Ji, V., 2015. A first-principles study on gas sensing properties of graphene and Pd-doped graphene. Appl. Surf. Sci. 343, 121–127.
Madhusudan, P., Wageh, S., Al-Ghamdi, A.A., Zhang, J., Cheng, B., Yu, Y., 2020. Graphene-Zn0.5Cd0.5S nanocomposite with enhanced visible-light photocatalytic CO_2 reduction activity. Appl. Surf. Sci. 506, 144683.
Magne, T.M., de Oliveira Vieira, T., Alencar, L.M.R., Junior, F.F.M., Gemini-Piperni, S., Carneiro, S.V., Fechine, L.M.U.D., Freire, R.M., Golokhvast, K., Metrangolo, P., Fechine, P.B.A., Santos-Oliveira, R., 2021. Graphene and its derivatives:

understanding the main chemical and medicinal chemistry roles for biomedical applications. J. Nanostruct. Chem. https://doi.org/10.1007/s40097-021-00444-3.
Mahalingam, S., Manap, A., Omar, A., Low, F.W., Afandi, N., Chia, C.H., Abd Rahim, N., 2021. Functionalized graphene quantum dots for dye-sensitized solar cell: key challenges, recent developments and future prospects. Renew. Sustain. Energy Rev. 144, 110999.
Maharubin, S., Zhang, X., Zhu, F., Zhang, H.-C., Zhang, G., Zhang, Y., 2016. Synthesis and applications of semiconducting graphene. J. Nanomater., 6375962 https://doi.org/10.1155/2016/6375962.
Mahdiani, M., Soofivand, F., Ansari, F., Salavati-Niasari, M., 2018. Grafting of CuFe12O19 nanoparticles on CNT and graphene: eco-friendly synthesis, characterization and photocatalytic activity. J. Clean. Prod. 176, 1185–1197.
Malinga, N.N., Jarvis, A.L.L., 2020. Synthesis, characterization and magnetic properties of Ni, Co and FeCo nanoparticles on reduced graphene oxide for removal of Cr(VI). J. Nanostruct. Chem. 10 (1), 55–68.
Moon, D.-B., Bag, A., Lee, H.-B., Meeseepong, M., Lee, D.-H., Lee, N.-E., 2021. A stretchable, room-temperature operable, chemiresistive gas sensor using nanohybrids of reduced graphene oxide and zinc oxide nanorods. Sensor. Actuator. B Chem. 345, 130373.
Nagarajan, L., Saravanan, P., Kumaraguru, K., Joo, S.-W., Vasseghian, Y., Rajeshkannan, R., Rajasimman, M., 2022. Synthesis of magnesium nanocomposites decked with multilayer graphene (MG) and its application for the adsorptive removal of pollutant. Chemosphere 298, 134121.
Naik, S.S., Lee, S.J., Begildayeva, T., Yu, Y., Lee, H., Choi, M.Y., 2020. Pulsed laser synthesis of reduced graphene oxide supported ZnO/Au nanostructures in liquid with enhanced solar light photocatalytic activity. Environ. Pollut. 266, 115247.
Nidheesh, P.V., 2017. Graphene-based materials supported advanced oxidation processes for water and wastewater treatment: a review. Environ. Sci. Pollut. Control Ser. 24 (35), 27047–27069.
Oswal, P., Arora, A., Singh, S., Nautiyal, D., Kumar, S., Kumar, A., 2022. Functionalization of Graphene Oxide with a hybrid P, N ligand for immobilizing and stabilizing economical and non− toxic nanosized CuO: an efficient, robust and reusable catalyst for C− O coupling reaction in O-arylation of phenol. New J. Chem. 46, 3578–3587.
Pan, F., Li, B., Sarnello, E., Fei, Y., Feng, X., Gang, Y., Xiang, X., Fang, L., Li, T., Hu, Y.H., 2020. Pore-edge tailoring of single-atom iron–nitrogen sites on graphene for enhanced CO_2 reduction. ACS Catal. 10 (19), 10803–10811.
Park, Y., Kang, S.-H., Choi, W., 2011. Exfoliated and reorganized graphite oxide on titania nanoparticles as an auxiliary co-catalyst for photocatalytic solar conversion. Phys. Chem. Chem. Phys. 13 (20), 9425–9431.
Pastrana-Martínez, L., Silva, A., Fonseca, N., Vaz, J., Figueiredo, J., Faria, J., 2016. Photocatalytic reduction of CO_2 with water into methanol and ethanol using graphene derivative–TiO_2 composites: effect of pH and copper (I) oxide. Top. Catal. 59 (15), 1279–1291.
Pham, T.V., Kim, J.-G., Jung, J.Y., Kim, J.H., Cho, H., Seo, T.H., Lee, H., Kim, N.D., Kim, M.J., 2019. High areal capacitance of N-doped graphene synthesized by arc discharge. Adv. Funct. Mater. 29 (48), 1905511.
Pham, V.H., Cuong, T.V., Nguyen-Phan, T.-D., Pham, H.D., Kim, E.J., Hur, S.H., Shin, E. W., Kim, S., Chung, J.S., 2010. One-step synthesis of superior dispersion of chemically converted graphene in organic solvents. Chem. Commun. 46 (24), 4375–4377.
Phan, P.Q., Chae, S., Pornaroontham, P., Muta, Y., Kim, K., Wang, X., Saito, N., 2020. In situ synthesis of copper nanoparticles encapsulated by nitrogen-doped graphene at room temperature via solution plasma. RSC Adv. 10 (60), 36627–36635.
Quan, B., Jin, A., Yu, S.H., Kang, S.M., Jeong, J., Abruña, H.D., Jin, L., Piao, Y., Sung, Y. E., 2018. Solvothermal-derived S-doped graphene as an anode material for sodium-ion batteries. Adv. Sci. 5 (5), 1700880.
Raccichini, R., Varzi, A., Passerini, S., Scrosati, B., 2015. The role of graphene for electrochemical energy storage. Nat. Mater. 14 (3), 271–279.
Raja, A., Rajasekaran, P., Selvakumar, K., Arunpandian, M., Kaviyarasu, K., Bahadur, S. A., Swaminathan, M., 2020. Visible active reduced graphene oxide-$BiVO_4$-ZnO ternary photocatalyst for efficient removal of ciprofloxacin. Separ. Purif. Technol. 233, 115996.
Razaq, A., Bibi, F., Zheng, X., Papadakis, R., Jafri, S.H.M., Li, H., 2022. Review on graphene-, graphene oxide-, reduced graphene oxide-based flexible composites: from fabrication to applications. Materials 15 (3), 1012.
Rezaul Karim, K.M., Tarek, M., Ong, H.R., Abdullah, H., Yousuf, A., Cheng, C.K., Khan, M.M.R., 2019. Photoelectrocatalytic reduction of carbon dioxide to methanol using $CuFe_2O_4$ modified with graphene oxide under visible light irradiation. Ind. Eng. Chem. Res. 58 (2), 563–572.
Sadegh, F., Politakos, N., de San Roman, E.G., Sanz, O., Modarresi-Alam, A.R., Tomovska, R., 2021. Toward enhanced catalytic activity of magnetic nanoparticles integrated into 3D reduced graphene oxide for heterogeneous Fenton organic dye degradation. Sci. Rep. 11 (1), 1–16.
Saleh, T.A., Al-Hammadi, S.A., 2021. A novel catalyst of nickel-loaded graphene decorated on molybdenum-alumina for the HDS of liquid fuels. Chem. Eng. J. 406, 125167.
Sarkar, A.K., Yun, Y.S., 2021. Role of adsorptive concentration in fenton-like degradation of organic pollutants by biopolymeric FeOOH/graphene oxide composite catalyst: proof of concept. Adv. Sustain. Syst. 5 (9), 2100060.
Scheuermann, G.M., Rumi, L., Steurer, P., Bannwarth, W., Mülhaupt, R., 2009. Palladium nanoparticles on graphite oxide and its functionalized graphene derivatives as highly active catalysts for the Suzuki− Miyaura coupling reaction. J. Am. Chem. Soc. 131 (23), 8262–8270.
Shandilya, P., Mittal, D., Soni, M., Raizada, P., Hosseini-Bandegharaei, A., Saini, A.K., Singh, P., 2018. Fabrication of fluorine doped graphene and $SmVO_4$ based dispersed and adsorptive photocatalyst for abatement of phenolic compounds from water and bacterial disinfection. J. Clean. Prod. 203, 386–399.
Shao, L., Jiang, D., Xiao, P., Zhu, L., Meng, S., Chen, M., 2016. Enhancement of g-C_3N_4 nanosheets photocatalysis by synergistic interaction of ZnS microsphere and RGO inducing multistep charge transfer. Appl. Catal. B Environ. 198, 200–210.
Sharma, S., Pollet, B.G., 2012. Support materials for PEMFC and DMFC electrocatalysts—a review. J. Power Sources 208, 96–119.
Shen, B., Chen, J., Yan, X., Xue, Q., 2012. Synthesis of fluorine-doped multi-layered graphene sheets by arc-discharge. RSC Adv. 2 (17), 6761–6764.
Shi, P., Su, R., Wan, F., Zhu, M., Li, D., Xu, S., 2012. Co_3O_4 nanocrystals on graphene oxide as a synergistic catalyst for degradation of Orange II in water by advanced oxidation technology based on sulfate radicals. Appl. Catal. B Environ. 123–124, 265–272.
Shyamala, R., Devi, L.G., 2020. Reduced graphene oxide/SnO_2 nanocomposites for the photocatalytic degradation of rhodamine B: preparation, characterization, photosensitization, vectorial charge transfer mechanism and identification of reaction intermediates. Chem. Phys. Lett. 748, 137385.
Son, M., Chee, S.-S., Kim, S.-Y., Lee, W., Kim, Y.H., Oh, B.-Y., Hwang, J.Y., Lee, B.H., Ham, M.-H., 2020. High-quality nitrogen-doped graphene films synthesized from pyridine via two-step chemical vapor deposition. Carbon 159, 579–585.
Srivastava, S., Pal, P., Sharma, D.K., Kumar, S., Senguttuvan, T.D., Gupta, B.K., 2022. Ultrasensitive boron–nitrogen-codoped CVD graphene-derived NO_2 gas sensor. ACS Mater. Au 2 (3), 356–366.
Stankovich, S., Dikin, D., Piner, R., Kohlhaas, K., Kleinhammes, A., Jia, Y., Wu, Y., Nguyen, S., Ruoff, R., Synthesis of graphene-based nanosheets via chemical reduction of exfoliated graphite oxide. Carbon 45 (7), 1558-1565.
Su, P., Zhou, M., Lu, X., Yang, W., Ren, G., Cai, J., 2019. Electrochemical catalytic mechanism of N-doped graphene for enhanced H_2O_2 yield and in-situ degradation of organic pollutant. Appl. Catal. B Environ. 245, 583–595.
Sun, Y., Liu, X., Lv, X., Wang, T., Xue, B., 2021. Synthesis of novel lignosulfonate-modified graphene hydrogel for ultrahigh adsorption capacity of Cr (VI) from wastewater. J. Clean. Prod. 295, 126406.
Trapalis, A., Todorova, N., Giannakopoulou, T., Boukos, N., Speliotis, T., Dimotikali, D., Yu, J., 2016. TiO2/graphene composite photocatalysts for NOx removal: a comparison of surfactant-stabilized graphene and reduced graphene oxide. Appl. Catal. B Environ. 180, 637–647.
Ullah, S., Liu, Y., Hasan, M., Zeng, W., Shi, Q., Yang, X., Fu, L., Ta, H.Q., Lian, X., Sun, J., Yang, R., Liu, L., Rümmeli, M.H., 2022. Direct synthesis of large-area Al-doped graphene by chemical vapor deposition: advancing the substitutionally doped graphene family. Nano Res. 15 (2), 1310–1318.
Valencia, A.M., Valencia, C.H., Zuluaga, F., Grande-Tovar, C.D., 2021. Synthesis and fabrication of films including graphene oxide functionalized with chitosan for regenerative medicine applications. Heliyon 7 (5), e07058.
Vasseghian, Y., Dragoi, E.-N., Almomani, F., Le, V.T., 2022. Graphene-based materials for metronidazole degradation: a comprehensive review. Chemosphere 286, 131727.
Vatandost, E., Ghorbani-HasanSaraei, A., Chekin, F., Raeisi, S.N., Shahidi, S.-A., 2020. Green tea extract assisted green synthesis of reduced graphene oxide: application for highly sensitive electrochemical detection of sunset yellow in food products. Food Chem. X 6, 100085.
Verma, M.L., Sukriti, Dhanya, B.S., Saini, R., Das, A., Varma, R.S., 2022. Synthesis and application of graphene-based sensors in biology: a review. Environ. Chem. Lett. https://doi.org/10.1007/s10311-022-01404-1.
Wadekar, P.H., Ahirrao, D.J., Khose, R.V., Pethsangave, D.A., Jha, N., Some, S., 2018. Synthesis of aqueous dispersible reduced graphene oxide by the reduction of graphene oxide in presence of carbonic acid. ChemistrySelect 3 (20), 5630–5638.
Wan, Z., Wang, J., 2017. Degradation of sulfamethazine using Fe3O4-Mn3O4/reduced graphene oxide hybrid as Fenton-like catalyst. J. Hazard Mater. 324, 653–664.
Wang, C., Chen, Q., Guo, T., Li, Q., 2020. Environmental effects and enhancement mechanism of graphene/tourmaline composites. J. Clean. Prod. 262, 121313.
Wang, C., Shi, P., Cai, X., Xu, Q., Zhou, X., Zhou, X., Yang, D., Fan, J., Min, Y., Ge, H., Yao, W., 2016. Synergistic effect of Co_3O_4 nanoparticles and graphene as catalysts for peroxymonosulfate-based orange II degradation with high oxidant utilization efficiency. J. Phys. Chem. C 120 (1), 336–344.
Wang, J., Duan, X., Dong, Q., Meng, F., Tan, X., Liu, S., Wang, S., 2019. Facile synthesis of N-doped 3D graphene aerogel and its excellent performance in catalytic degradation of antibiotic contaminants in water. Carbon 144, 781–790.
Wang, X., Li, X., Zhang, L., Yoon, Y., Weber, P.K., Wang, H., Guo, J., Dai, H., 2009. N-doping of graphene through electrothermal reactions with ammonia. Science 324 (5928), 768–771.
Wani, A.A., Khan, A.M., Manea, Y.K., Shahadat, M., Ahammad, S.Z., Ali, S.W., 2020. Graphene-supported organic-inorganic layered double hydroxides and their environmental applications: a review. J. Clean. Prod. 273, 122980.
Wei, Z., Pan, R., Hou, Y., Yang, Y., Liu, Y., 2015. Graphene-supported Pd catalyst for highly selective hydrogenation of resorcinol to 1, 3-cyclohexanedione through giant π-conjugate interactions. Sci. Rep. 5 (1), 1–9.
Wu, D., Wang, T., Wang, L., Jia, D., 2019. Hydrothermal synthesis of nitrogen, sulfur co-doped graphene and its high performance in supercapacitor and oxygen reduction reaction. Microporous Mesoporous Mater. 290, 109556.
Wu, W., Song, Y., Bai, L., Chen, Z., Sun, H., Zhen, G., Zhan, R., Shen, Y., Qian, J., Yuan, Q., 2020. Graphene oxide-BiOCl nanoparticle composites as catalysts for oxidation of volatile organic compounds in nonthermal plasmas. ACS Appl. Nano Mater. 3 (9), 9363–9374.
Wu, Z., Ambrožová, N., Eftekhari, E., Aravindakshan, N., Wang, W., Wang, Q., Zhang, S., Kočí, K., Li, Q., 2019. Photocatalytic H_2 generation from aqueous ammonia solution using TiO_2 nanowires-intercalated reduced graphene oxide composite membrane under low power UV light. Emergentes Mater. 2 (3), 303–311.

Xu, M., Hu, X., Wang, S., Yu, J., Zhu, D., Wang, J., 2019. Photothermal effect promoting CO_2 conversion over composite photocatalyst with high graphene content. J. Catal. 377, 652–661.
Yam, K.M., Guo, N., Jiang, Z., Li, S., Zhang, C., 2020. Graphene-based heterogeneous catalysis: role of graphene. Catalysts 10 (1), 53.
Yan, Y., Shin, W.I., Chen, H., Lee, S.-M., Manickam, S., Hanson, S., Zhao, H., Lester, E., Wu, T., Pang, C.H., 2021. A recent trend: application of graphene in catalysis. Carbon Lett. 31 (2), 177–199.
Yang, L., Li, Z., Jiang, H., Jiang, W., Su, R., Luo, S., Luo, Y., 2016. Photoelectrocatalytic oxidation of bisphenol A over mesh of TiO_2/graphene/Cu_2O. Appl. Catal. B Environ. 183, 75–85.
Yeom, D.-Y., Jeon, W., Tu, N.D.K., Yeo, S.Y., Lee, S.-S., Sung, B.J., Chang, H., Lim, J.A., Kim, H., 2015. High-concentration boron doping of graphene nanoplatelets by simple thermal annealing and their supercapacitive properties. Sci. Rep. 5 (1), 1–10.
Yin, Z., Cui, C., Chen, H., Yu, X., Qian, W., 2020. The application of carbon nanotube/graphene-based nanomaterials in wastewater treatment. Small 16 (15), 1902301.
Zaera, F., 2022. Designing sites in heterogeneous catalysis: are we reaching selectivities competitive with those of homogeneous catalysts? Chem. Rev. 122 (9), 8594–8757.
Zan, R., Altuntepe, A., Erkan, S., 2021. Substitutional boron doping of graphene using diborane in CVD. Phys. E Low-dimens. Syst. Nanostruct. 128, 114629.
Zhang, S., Kang, P., Meyer, T.J., 2014. Nanostructured tin catalysts for selective electrochemical reduction of carbon dioxide to formate. J. Am. Chem. Soc. 136 (5), 1734–1737.
Zhang, X., Sun, Y., Cui, X., Jiang, Z., 2012. A green and facile synthesis of TiO_2/graphene nanocomposites and their photocatalytic activity for hydrogen evolution. Int. J. Hydrogen Energy 37 (1), 811–815.
Zhou, J., Wang, Z., Yang, D., Zhang, W., Chen, Y., 2019. Free-standing S, N co-doped graphene/Ni foam as highly efficient and stable electrocatalyst for oxygen evolution reaction. Electrochim. Acta 317, 408–415.
Zhuang, S., Nunna, B.B., Boscoboinik, J.A., Lee, E.S., 2017. Nitrogen-doped graphene catalysts: high energy wet ball milling synthesis and characterizations of functional groups and particle size variation with time and speed. Int. J. Energy Res. 41 (15), 2535–2554.
Zhuo, Q., Zhang, Y., Du, Q., Yan, C., 2015. Facile reduction of graphene oxide at room temperature by ammonia borane via salting out effect. J. Colloid Interface Sci. 457, 243–247.